
Addis Ababa University
Addis Ababa Institute of Technology
School of Electrical and Computer Engineering

# V/F CONTROL DESIGN AND SIMULATION FOR FIVE-PHASE INDUCTION MOTOR

A thesis submitted to Addis Ababa Institute of Technology, School of Graduate Studies, Addis Ababa University

In partial fulfillment of the requirement for the Degree of Master of Science in Electrical Engineering (*Electrical Control Engineering*)

By

Mesfin Tilahune Tessema

Advisor: Dr. Mengesha Mamo

ADDIS ABABA, ETHIOPIA
MARCH 2015


Addis Ababa University
Addis Ababa Institute of Technology
School of Electrical and Computer Engineering

# V/F CONTROL DESIGN AND SIMULATION FOR FIVE-PHASE INDUCTION MOTOR

By Mesfin Tilahune Tessema

APPROVED BY BOARD OF EXAMINERS

| | |
|---|---|
| Dean, School of Graduate Committee | Signature |
| Dr. Mengesha Mamo<br>Advisor | Signature |
| Internal Examiner | Signature |
| External Examiner | Signature |

## Acknowledgments

I would like to express my deepest gratitude to my research advisor Dr.Mengesha Mamo, without his generous and constant support, I could not finish my study program in control Engineering. My family and I are greatly indebted to him.

Also, I would like to thank all the people around me in the *AAiT* for their friendship and help. They made my stay at *AAiT* a memorable one. Finally, I wouldn't have been in this position if I hadn't had the support and best wishes from my family, especially my parents to whom I owe everything.

# Table of Contents

# List of Figures

# List of Tables

## List of Abbreviations

| | | |
|---|---|---|
| PWM | …….. | Pulse Width Modulation |
| SVPWM | …….. | Space Vector Pulse Width Modulation |
| PI | …….. | Proportional Integral |
| IGBT | …….. | Insulated Gate Bipolar Transistor |
| DC | …….. | Direct Current |
| AC | …….. | Alternating Current |

## List of Notations

V: Voltage

I: Current

Ψ: Flux linkage

R: Resistance

L: Inductance

M: Magnetizing inductance (per phase)

P: Number of pole pairs

$T_e$: Torque developed by the machine

$T_L$: Load torque

J: Inertia

p: Differential operator

$T_r$: Rotor time constant

ω: Rotational speed of the rotor with respect to the stator

$\omega_a$: Rotational speed of the d-axis of the arbitrary common reference frame

$\omega_r$: Rotational speed of the rotor flux space vector with respect to the stator

$\omega_{sl}$: Slip speed

θ: Instantaneous position of the magnetic axis of the rotor phase 'a' with respect to the stationary magnetic axis of the stator phase 'a'

$\theta_s$ : Instantaneous angular position of the d-axis of the common reference frame with respect to the phase 'a' magnetic axis of the stator

$\theta_r$ : Instantaneous angular position of the d-axis of the common reference frame with respect to the phase 'a' magnetic axis of the rotor

$\varphi_r$ : Instantaneous angular position of the rotor flux with respect to the phase "a" magnetic axis of the stator

$A_s$: Transformation matrix applied to stator quantities

$A_r$: Transformation matrix applied to rotor quantities

C: Decoupling (Clark's) transformation matrix

## Abstract

Multi-phase machine and drives is a topic of growing relevance in recent years, and it presents many challenging issues that still need further research. Numerous industrial applications, such as textile industry, paper mills, robotics and railway traction, require multi-phase electric drive.

This Thesis work discussed a comprehensive simulation model of a five-phase induction motor drive system. Both open loop and closed-loop control is elaborated. Also, discussed the advantages of a drive system and identified its potential application areas. Modeling of a five-phase voltage source inverter was illustrated for step mode of operation and SVPWM mode of operation. This was followed by the phase variable model of a five-phase induction motor. The model was then transformed into two orthogonal planes, namely d-q, x-y and the torque equation is obtained. The scalar control principle was then presented for the five-phase induction motor drive system. The difference between the scalar control principle applied to a three-phase system and a five-phase system is highlighted.

Finally, the complete component modeling is developed using 'simpower system' blocksets of Matlab/Simulink. To address the real time implementation issues, dead banding of the inverter switches are also incorporated in the simulation model.



***(Key words: Ten-step mode, SVPWM, V/F speed control, phase variable model, PI controller, x-y plane, d-q plane, Clark transformation, Park transformation)***

# CHAPTER 1

## INTRODUCTION

### 1.1 Background

More than half of the total electrical energy produced in developed countries is converted into mechanical energy in electric motors, freeing the society from the tedious burden of physical labor. Among many types of the motors, three-phase induction machines still enjoy the same unparalleled popularity as they did a century ago. At least 90% of industrial drive systems employ induction motors. Most of the motors are uncontrolled, but the share of adjustable speed induction motor drives fed from power electronic converters is steadily increasing, phasing out dc drives. It is estimated that more than 50 billion dollars could be saved annually by replacing all ‘‘dumb’’ motors with controlled ones [1-2]. However, control of induction machines is a much more challenging task than control of dc motors.

The induction motor control methods can be broadly classified into scalar and vector control. In the scalar control only the magnitude and frequency of voltage, current and flux linkage space vectors are controlled. In contrast in vector control not only magnitude and frequency but also instantaneous positions of voltage, current and flux space vectors are controlled [6]. Thus in vector control scheme the controller acts on the position of the space vectors and provides their correct orientation for both steady state and transient condition.

However, with the advent of cheap and fast switching power electronics devices not only the control of induction machine became easier and flexible but also the number of phases of machine became a design parameter. Multi-phase machines (more than three-phases) are found to possess several advantages over three-phase machines such as lower torque pulsation, higher torque density, fault tolerance, stability and lower current ripple[4]. Thus multi-phase order machines are normally considered for niche application areas such as ship propulsion, ‘more electric aircraft’, and electric/hybrid electric vehicles etc.

### 1.2 Problem Description

In numerous industrial applications, the dynamic performance of the drive is not so important especially where sudden change in speed is not required. In such cases the cheap solution is to

use open-loop or closed-loop constant v/f control scheme. Induction motors have well known advantages of simple construction, reliability, ruggedness, low maintenance and low cost which has led to their wide spread use in many industrial applications. The major problem of this machine is their complicated control for speed regulation in industrial drive applications. Two major difficulties are the necessity of providing adjustable-frequency voltage (dc motors are controlled by adjusting the magnitude of supply voltage) and the nonlinearity and complexity of analytical model of the motor, aggrandized by parameter uncertainty.

## 1.3 Objectives of the Thesis

### 1.3.1 General Objective

Motivated by the above mentioned limitations, the main objective of this thesis work is to investigate the performance of closed-loop constant V/F control scheme for five-phase induction motor.

### 1.3.2 Specific Objectives

Specifically, considering five phase closed loop V/F control scheme, the objectives of this thesis work are:

- Studying different dynamic models of five-phase induction motor and five phase inverter schemes employed in closed loop speed control systems.
- To incorporate a dead band generators for the five phase inverter switches in the simulation model.
- Propose an effective controlling algorithm sequence for multi-phase induction motor systems.
- To investigate the complexity versus performance improvement trade-off between five phase drive system and three phase drive system.

## 1.4 Contribution of the Thesis

In all the literatures seen so far in section (2.5), five phase induction motor drive system has been investigated at various levels. However, some of the differences in the previous work and the current research are underlined in the following points.

- Unlike the previous works mentioned in chapter two the closed loop V/F drive system is fully implemented.

- SVPWM is implemented for four neighboring active vectors instead of two active vectors.
- The advantage of multi-phase motors are shown clearly.

## 1.5 Outline of the Thesis

In this thesis, the phase variable model technique will be proposed for V/F control of five phase induction motor. With the phase variable model, a five-phase induction machine is constructed using ten phase belts, each of 36 degrees, along the circumference of the stator. The spatial displacement between phases is therefore 72 degrees. The rotor winding is treated as an equivalent five-phase winding, with the same properties as the stator winding. It is assumed that the rotor winding has already been referred to as stator winding, using the winding transformation ratio.

The reminder of the thesis is organized as follows:

**Chapter II** over view of five phase induction motor is described. Specifically: Multi phase induction motor, five phase induction motor and mathematical analysis of five phase induction motor models, d-q Transformation and mathematical analysis of five phase inverter are explained in detail.

**Chapter III** a comprehensive review of methodology is taking place.

**Chapter IV** presents elaborated analysis of PI and V/F controller for five phase induction motor.

**Chapter V** compares the theoretical results with the simulation results to verify the quit nature and stable operation of proposed five phase induction motor drive.

Finally, **Chapter VI** draws the conclusions from the work done in this thesis and discusses further research possible in the future.

# CHAPTER TWO

## FIVE-PHASE INDUCTION MOTOR

### 2.1 Introduction

Three phase electrical power is readily available as the power is generated, transmitted, and distributed in three phases. This is the most optimal number of phases for generation and transmission, as the tradeoff exists between the complexity and power handling capability of the three-phase system. The variable speed electric drive is also developed for three-phase AC machines. However, a power electronic converter, most commonly a voltage source or current source inverter, is invariably used to supply such three-phase drives. The power electronic converters do not pose any limit on their number of legs. The number of output phases in an inverter is the same as their respective number of legs. Hence, adding an additional leg to an inverter increases the number of output phases [6]. This degree of freedom lead to interest in developing variable speed electric drives with more than three phases. The first proposal of a variable speed five-phase induction motor drive is believed to have been made in 1969 [1]. The five-phase inverter used initially operated in the square wave mode; however, later the pulse width modulation (PWM) mode of operation was used. Six-phase drives have attracted much attention in the literature, after their advantages were revealed in 1983 [2]. The research on high phase order motor drives remained steady until the end of the 19th century. The multi-phase drive attracted much attention from researchers after the advent of cheap and reliable power switching devices, as well as powerful digital signal processors.

### 2.2 Mathematical Model of Five Phase Induction Motor

The model of a five-phase induction motor described is developed initially in phase variable form. In order to simplify the model by removing the time variation of inductance terms, a transformation is applied and a so-called d-q-x-y-0 model of the machine is constructed. It is assumed that the spatial distribution of all the magneto-motive forces (fields) in the machine is sinusoidal, since only torque production due to the 1st harmonic of the field is considered. However, in a five-phase machine with concentrated type of winding, the 3rd harmonic component of the current is also used together with the fundamental to enhance the torque production.

### 2.2.1 Phase Variable Model

A five-phase induction machine is constructed using ten phase belts, each of 36 degrees, along the circumference of the stator. The spatial displacement between phases is therefore 72 degrees. The rotor winding is treated as an equivalent five-phase winding, with the same properties as the stator winding. It is assumed that the rotor winding has already been referred to as stator winding, using the winding transformation ratio. A five-phase induction machine can then be described with the following voltage equilibrium and flux linkage equations in matrix form (underlined symbols):

$$\underline{v}^{s}_{abcde} = R_s \underline{i}^{s}_{abcde} + \frac{d\underline{\psi}^{s}_{abcde}}{dt} \tag{2.1}$$

$$\underline{\psi}^{s}_{abcde} = L_s \underline{i}^{s}_{abcde} + L_{sr} \underline{i}^{r}_{abcde} \tag{2.2}$$

$$\underline{v}^{r}_{abcde} = R_s \underline{i}^{r}_{abcde} + \frac{d\underline{\psi}^{r}_{abcde}}{dt} \tag{2.3}$$

$$\underline{\psi}^{r}_{abcde} = L_s \underline{i}^{r}_{abcde} + L_{sr} \underline{i}^{s}_{abcde} \tag{2.4}$$

The following definition of phase voltages, currents and flux linkages applies to equations:

$$\underline{v}^{s}_{abcde} = \begin{bmatrix} v_{as} & v_{bs} & v_{cs} & v_{ds} & v_{es} \end{bmatrix}^T \tag{2.5}$$

$$\underline{i}^{s}_{abcde} = \begin{bmatrix} i_{as} & i_{bs} & i_{cs} & i_{ds} & i_{es} \end{bmatrix}^T \tag{2.6}$$

$$\underline{\psi}^{s}_{abcde} = \begin{bmatrix} \psi_{as} & \psi_{bs} & \psi_{cs} & \psi_{ds} & \psi_{es} \end{bmatrix}^T \tag{2.7}$$

$$\underline{v}^{r}_{abcde} = \begin{bmatrix} v_{ar} & v_{br} & v_{cr} & v_{dr} & v_{er} \end{bmatrix}^T \tag{2.8}$$

$$\underline{i}^{r}_{abcde} = \begin{bmatrix} i_{ar} & i_{br} & i_{cr} & i_{dr} & i_{er} \end{bmatrix}^T \tag{2.9}$$

$$\underline{\psi}^{r}_{abcde} = \begin{bmatrix} \psi_{ar} & \psi_{br} & \psi_{cr} & \psi_{dr} & \psi_{er} \end{bmatrix}^T \tag{2.10}$$

The matrices of stator and rotor inductances are given with ($\alpha=\pi/5$):

$$\underline{L}_s = \begin{bmatrix} L_{aas} & L_{abs} & L_{acs} & L_{ads} & L_{aes} \\ L_{abs} & L_{bbs} & L_{bcs} & L_{bds} & L_{bes} \\ L_{acs} & L_{bcs} & L_{ccs} & L_{cds} & L_{ces} \\ L_{ads} & L_{bds} & L_{cds} & L_{dds} & L_{des} \\ L_{aes} & L_{bes} & L_{ces} & L_{des} & L_{ees} \end{bmatrix} \tag{2.11}$$

$$\underline{L}_s = \begin{bmatrix} L_{ls}+M & M\cos\alpha & M\cos\alpha & M\cos 2\alpha & M\cos\alpha \\ M\cos\alpha & L_{ls}+M & M\cos\alpha & M\cos 2\alpha & M\cos 2\alpha \\ M\cos 2\alpha & M\cos\alpha & L_{ls}+M & M\cos\alpha & M\cos 2\alpha \\ M\cos 2\alpha & M\cos 2\alpha & M\cos\alpha & L_{ls}+M & M\cos\alpha \\ M\cos\alpha & M\cos 2\alpha & M\cos 2\alpha & M\cos\alpha & L_{ls}+M \end{bmatrix} \tag{2.12}$$

$$\underline{\mathrm{L}}_{\mathrm{r}} = \begin{bmatrix} \mathrm{L}_{\mathrm{aar}} & \mathrm{L}_{\mathrm{abr}} & \mathrm{L}_{\mathrm{acr}} & \mathrm{L}_{\mathrm{adr}} & \mathrm{L}_{\mathrm{aer}} \\ \mathrm{L}_{\mathrm{abr}} & \mathrm{L}_{\mathrm{bbr}} & \mathrm{L}_{\mathrm{bcr}} & \mathrm{L}_{\mathrm{bdr}} & \mathrm{L}_{\mathrm{ber}} \\ \mathrm{L}_{\mathrm{acr}} & \mathrm{L}_{\mathrm{bcr}} & \mathrm{L}_{\mathrm{ccr}} & \mathrm{L}_{\mathrm{cdr}} & \mathrm{L}_{\mathrm{cer}} \\ \mathrm{L}_{\mathrm{adr}} & \mathrm{L}_{\mathrm{bdr}} & \mathrm{L}_{\mathrm{cdr}} & \mathrm{L}_{\mathrm{ddr}} & \mathrm{L}_{\mathrm{der}} \\ \mathrm{L}_{\mathrm{aes}} & \mathrm{L}_{\mathrm{bes}} & \mathrm{L}_{\mathrm{ces}} & \mathrm{L}_{\mathrm{des}} & \mathrm{L}_{\mathrm{ees}} \end{bmatrix} \tag{2.13}$$

$$\underline{L}_r = \begin{bmatrix} L_{lr}+M & M\cos\alpha & M\cos\alpha & M\cos 2\alpha & M\cos\alpha \\ M\cos\alpha & L_{lr}+M & M\cos\alpha & M\cos 2\alpha & M\cos 2\alpha \\ M\cos 2\alpha & M\cos\alpha & L_{lr}+M & M\cos\alpha & M\cos 2\alpha \\ M\cos 2\alpha & M\cos 2\alpha & M\cos\alpha & L_{lr}+M & M\cos\alpha \\ M\cos\alpha & M\cos 2\alpha & M\cos 2\alpha & M\cos\alpha & L_{lr}+M \end{bmatrix} \tag{2.14}$$

Mutual inductances between stator and rotor windings are given with:

$$\underline{L}_{sr} = M\begin{bmatrix} \cos\theta & \cos(\theta+\alpha) & \cos(\theta+2\alpha) & \cos(\theta-2\alpha) & \cos(\theta-\alpha) \\ \cos(\theta-\alpha) & \cos\theta & \cos(\theta+\alpha) & \cos(\theta+2\alpha) & \cos(\theta-2\alpha) \\ \cos(\theta-2\alpha) & \cos(\theta-\alpha) & \cos\theta & \cos(\theta+\alpha) & \cos(\theta+2\alpha) \\ \cos(\theta+2\alpha) & \cos(\theta-2\alpha) & \cos(\theta-\alpha) & \cos\theta & \cos(\theta+\alpha) \\ \cos(\theta+\alpha) & \cos(\theta+2\alpha) & \cos(\theta-2\alpha) & \cos(\theta-\alpha) & \cos\theta \end{bmatrix} \tag{2.15}$$

$$\underline{\mathrm{L}}_{\mathrm{rs}} = \underline{L}_{sr}^{T} \tag{2.16}$$

The angle $\theta$ denotes the instantaneous position of the magnetic axis of the rotor phase ‘a’ with respect to the stationary stator phase ’a’ magnetic axis.

$$\left.\begin{aligned} R_s &= \mathrm{diag}\left(R_S, R_S, R_S, R_S, R_S\right) \\ R_r &= \mathrm{diag}\left(R_r, R_r, R_r, R_r, R_r\right) \end{aligned}\right\} \tag{2.17}$$

Motor torque can be expressed in terms of phase variables as:

$$T_e = \frac{P}{2} \underline{i}^T \frac{d\underline{L}_{abcde}}{d\theta} \underline{i} = \frac{P}{2} \begin{bmatrix} \underline{i}^{s^T}_{abcde} & \underline{i}^{r^T}_{abcde} \end{bmatrix} \frac{d\underline{L}_{abcde}}{d\theta} \begin{bmatrix} \underline{i}^{s}_{abcde} \\ \underline{i}^{r}_{abcde} \end{bmatrix} \tag{2.18}$$

$$T_e = P \underline{i}^{s^T}_{abcde} \frac{d\underline{L}_{sr}}{d\theta} \underline{i}^{r}_{abcde} \tag{2.19}$$

Substitution of stator and rotor currents from equations (2.6 and 2.9) Yields the torque equation in developed form:

$$T_e = -PM \left\{ \begin{array}{c} \left(i_{as}i_{ar} + i_{bs}i_{br} + i_{cs}i_{cr} + i_{ds}i_{dr} + i_{es}i_{er}\right)\sin\theta + \left(i_{es}i_{ar} + i_{as}i_{br} + i_{bs}i_{cr} + i_{cs}i_{dr} + i_{ds}i_{er}\right)\sin\left(\theta+\alpha\right) + \\ \left(i_{ds}i_{ar} + i_{es}i_{br} + i_{as}i_{cr} + i_{bs}i_{dr} + i_{cs}i_{er}\right)\sin\left(\theta+2\alpha\right) + \left(i_{cs}i_{ar} + i_{ds}i_{br} + i_{es}i_{cr} + i_{as}i_{dr} + i_{bs}i_{er}\right) \\ \sin\left(\theta-2\alpha\right) + \left(i_{bs}i_{ar} + i_{cs}i_{br} + i_{ds}i_{cr} + i_{es}i_{dr} + i_{as}i_{er}\right)\sin\left(\theta-\alpha\right) \end{array} \right\} \tag{2.20}$$

### 2.2.2 Model Transformation

In order to simplify the model, it is necessary to apply a co-ordinate transformation, which will remove the time varying inductances. The co-ordinate transformation is used in the power invariant form. The following transformation matrix is therefore applied to the stator five-phase winding:

$$\underline{A}_s = \sqrt{\frac{2}{5}} \begin{bmatrix} \cos\theta_s & \cos(\theta_s-\alpha) & \cos(\theta_s-2\alpha) & \cos(\theta_s+2\alpha) & \cos(\theta_s+\alpha) \\ -\sin\theta_s & -\sin\left(\theta_s-\alpha\right) & -\sin\left(\theta_s-2\alpha\right) & -\sin\left(\theta_s+2\alpha\right) & -\sin\left(\theta_s+\alpha\right) \\ 1 & \cos(2\alpha) & \cos(4\alpha) & \cos(4\alpha) & \cos(2\alpha) \\ 0 & \sin(2\alpha) & \sin(4\alpha) & -\sin(4\alpha) & -\sin(2\alpha) \\ \frac{1}{\sqrt{2}} & \frac{1}{\sqrt{2}} & \frac{1}{\sqrt{2}} & \frac{1}{\sqrt{2}} & \frac{1}{\sqrt{2}} \end{bmatrix} \tag{2.21}$$

Transformation of the rotor variables is performed using the same transformation expression, except that $\theta_s$ is replaced by $\beta$, where $\beta = \theta_s - \theta$. Here, $\theta_s$ is the instantaneous angular position of the d-axis of the common reference frame with respect to the phase 'a' magnetic axis of the stator, while $\beta$ is the instantaneous angular position of the d-axis of the common reference frame with respect to the phase 'a' magnetic axis of the rotor. Hence the transformation matrix for rotor is:

$$\underline{A}_r = \sqrt{\frac{2}{5}}\begin{bmatrix} \cos\beta & \cos(\beta-\alpha) & \cos(\beta-2\alpha) & \cos(\beta+2\alpha) & \cos(\beta+\alpha) \\ -\sin\beta & -\sin(\beta-\alpha) & -\sin(\beta-2\alpha) & -\sin(\beta+2\alpha) & -\sin(\beta+\alpha) \\ 1 & \cos(2\alpha) & \cos(4\alpha) & \cos(4\alpha) & \cos(2\alpha) \\ 0 & \sin(2\alpha) & \sin(4\alpha) & -\sin(4\alpha) & -\sin(2\alpha) \\ \frac{1}{\sqrt{2}} & \frac{1}{\sqrt{2}} & \frac{1}{\sqrt{2}} & \frac{1}{\sqrt{2}} & \frac{1}{\sqrt{2}} \end{bmatrix} \quad (2.22)$$

The angles of transformation for stator quantities and for rotor quantities are related to the arbitrary speed of the selected common reference frame through

$$\theta_s = \int \omega_a dt \quad (2.23)$$

$$\beta = \theta_s - \theta = \int (\omega_a - \omega) dt \quad (2.24)$$

Where $\omega$ is the instantaneous electrical angular speed of rotation of the rotor. Correlation between original phase variables and new variables in the transformed domain is governed by the following transformation expressions:

| Stator side | Rotor side | |
|---|---|---|
| $\underline{v}^s_{dq} = \underline{A}_s \underline{v}^s_{abcde}$ | $\underline{v}^r_{dq} = \underline{A}_r \underline{v}^r_{abcde}$ | (2.25) |
| $\underline{i}^s_{dq} = \underline{A}_s \underline{i}^s_{abcde}$ | $\underline{i}^r_{dq} = \underline{A}_r \underline{i}^r_{abcde}$ | (2.26) |
| $\underline{\psi}^s_{dq} = \underline{A}_s \underline{\psi}^s_{abcde}$ | $\underline{\psi}^r_{dq} = \underline{A}_r \underline{\psi}^r_{abcde}$ | (2.27) |

Substituting equations (2.1) and (2.5) into equation (2.25) and the application of equations (2.21) and (2.22) yield the machine's voltage equations in the common reference frame where p=d/dt:

| Stator side | Rotor side | |
|---|---|---|
| $v_{ds} = R_s i_{ds} - \omega_a \psi_{qs} + p\psi_{ds}$ | $v_{dr} = R_r i_{dr} - (\omega_a - \omega)\psi_{qr} + p\psi_{dr}$ | (2.28) |
| $v_{qs} = R_s i_{qs} + \omega_a \psi_{ds} + p\psi_{qs}$ | $v_{qr} = R_r i_{qr} - (\omega_a - \omega)\psi_{dr} + p\psi_{qr}$ | (2.29) |
| $v_{xs} = R_s i_{xs} + p\psi_{xs}$ | $v_{xr} = R_r i_{xr} + p\psi_{xr}$ | (2.30) |
| $v_{ys} = R_s i_{ys} + p\psi_{ys}$ | $v_{yr} = R_r i_{yr} + p\psi_{yr}$ | (2.31) |

$$v_{0s} = R_s i_{0s} + p\psi_{0s} \qquad v_{0r} = R_r i_{0r} + p\psi_{0r} \tag{2.32}$$

Transformation of flux linkage equations (2.1) and (2.2) results in

$$\psi_{ds} = (L_{ls} + 2.5M)i_{ds} + 2.5Mi_{dr} \qquad \psi_{dr} = (L_{lr} + 2.5M)i_{dr} + 2.5Mi_{ds} \tag{2.33}$$

$$\psi_{qs} = (L_{ls} + 2.5M)i_{qs} + 2.5Mi_{qr} \qquad \psi_{qr} = (L_{lr} + 2.5M)i_{qr} + 2.5Mi_{qs} \tag{2.34}$$

$$\psi_{xs} = L_{ls} i_{xs} \qquad \psi_{xr} = L_{lr} i_{xr} \tag{2.35}$$

$$\psi_{ys} = L_{ls} i_{ys} \qquad \psi_{yr} = L_{lr} i_{yr} \tag{2.36}$$

$$\psi_{0s} = L_{ls} i_{0s} \qquad \psi_{0r} = L_{lr} i_{0r} \tag{2.37}$$

Introduction of the magnetizing inductance $\boldsymbol{L_m=2.5M}$ enables equations (2.33-2.37) to be written in the following form:

$$\psi_{ds} = (L_{ls} + L_m)i_{ds} + L_m i_{dr} \qquad \psi_{dr} = (L_{lr} + L_m)i_{dr} + L_m i_{ds} \tag{2.38}$$

$$\psi_{qs} = (L_{ls} + L_m)i_{qs} + L_m i_{qr} \qquad \psi_{qr} = (L_{lr} + L_m)i_{qr} + L_m i_{qs} \tag{2.39}$$

$$\psi_{xs} = L_{ls} i_{xs} \qquad \psi_{xr} = L_{lr} i_{xr} \tag{2.40}$$

$$\psi_{ys} = L_{ls} i_{ys} \qquad \psi_{yr} = L_{lr} i_{yr} \tag{2.41}$$

$$\psi_{0s} = L_{ls} i_{0s} \qquad \psi_{0r} = L_{lr} i_{0r} \tag{2.42}$$

Finally, transformation of the original torque equation (2.44) yields

$$T_e = \frac{5P}{2} M\left[i_{dr} i_{qs} - i_{ds} i_{qr}\right] \tag{2.43}$$

$$T_e = PL_m\left[i_{dr} i_{qs} - i_{ds} i_{qr}\right] \tag{2.44}$$

The mechanical equation of rotor motion is invariant under the transformation and is

$$\mathrm{T_e} - \mathrm{T_L} = \frac{\mathrm{J}}{\mathrm{P}} \frac{\mathrm{d}\omega}{\mathrm{dt}} \tag{2.45}$$

Where J is the inertia and P is the number of poles in machine.

The difference between a three-phase machine model and a five-phase machine model lies in the extra x-y set of components that exist only in a five-phase machine. However, this extra set are

non-flux and non-torque producing components. They simply add to the extra losses in the machine.

In a five-phase machine, the x-y components are decoupled from d-q components; also there is no coupling of x-y with the rotor circuit. This is true for an n-phase AC machine with sinusoidal distributed MMF and hence only one pair of components, i.e.d-q produces torque and the

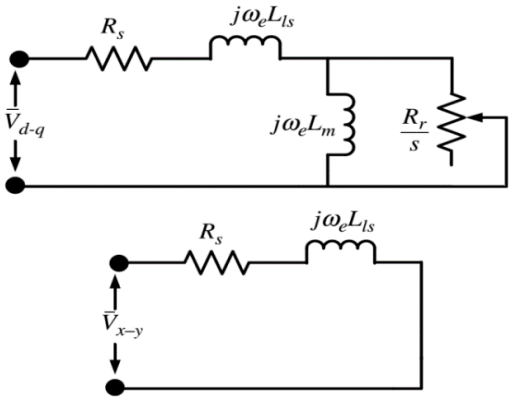


*Figure 2. 1: Steady-state equivalent circuit of a five-phase induction machine.*

Remaining component simply causes losses in the machine. Different harmonics of the stator voltage/current map into either the d-q or x-y planes of the stationary reference frame, depending on the harmonic order, as shown in. This is a general property of multi-phase systems, which lead to distinctions with respect to control of a multi-phase machine.

Thus the fundamental, 9th, 11th...are produced due to d-q components, while 3rd, 7th,13th...are generated due to x-y components and a multiple of the 5th harmonic is produced due to zero-sequence components. Harmonic mapping for five-phase machine is shown below:

| Component | Five-phase system |
|---|---|
| d-q | **$10j \pm 1$(j=0,1,2,…)** |
| x-y | **$10j \pm 3$(j=0,1,2,…)** |
| Zero sequence | **$10j \pm 5$(j=0,1,2,…)** |

*Table 2. 1: Harmonic mapping*

### 2.3 Five-Phase Two-Level Voltage Source Inverter Model

A five phase inverter has a similar front-side converter structure to that of a three-phase voltage source inverter. The fixed voltage and fixed frequency grid supply voltage is converted to DC by using either controlled (thyristor based or power transistor based) or uncontrolled rectifier (diode based). The output of the rectifier (AC-DC converter) is filtered to remove the ripple in the output voltage signal. The rectified and filtered DC voltage is fed to the inverter (DC-AC) block. The inverter block outputs five-phase variable voltage and variable frequency supply to feed motor drives or other applications as desired. The five-phase inverter has two additional legs when compared to a three-phase inverter. The rectifier, filter, and five-phase inverter constitute the complete three-phase fixed voltage and fixed frequency to five-phase variable voltage and variable frequency supply system. The power circuit topology of a five-phase voltage source inverter is shown in Figure (2.3). This was first proposed by [1]. Each switch in the circuit consists of two power semiconductor devices connected in anti-parallel. One of these is a fully controllable semiconductor, such as a bipolar transistor, MOSFET, or IGBT, while the second is a diode. The input of the inverter is a DC voltage, which is regarded as constant. The inverter outputs are denoted in Figure(2.3) with lower-case letters (a,b,c,d,e), while the points of connection of the outputs to the inverter legs have symbols in capital letters (A,B,C,D,E). The voltage of this point of connection is called the 'Pole voltage' or 'Leg voltage.' The voltage between the terminal of the output of the inverter and the neutral of the load is called the 'Phase voltage'. The voltage between the neutral of the load and the neutral of the DC link is called 'Common mode voltage'. The voltage across the two output terminals of the load is called the 'Line voltages'. However, in a five phase system, there exist two different line voltages, called non-adjacent and adjacent line voltages, contrary to a three-phase system where only one line voltage is defined.

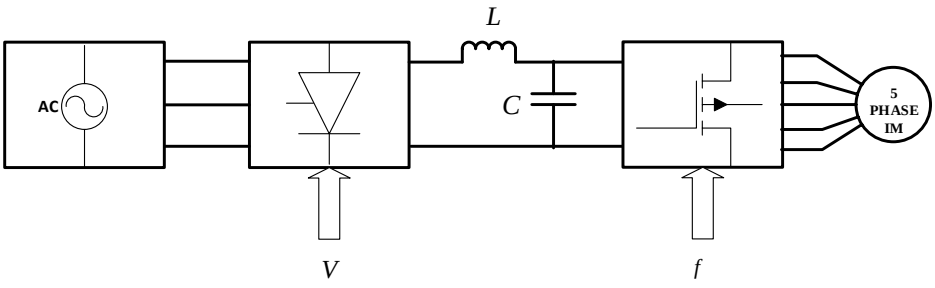


*Figure 2. 2: Block diagram of five-phase induction motor drive*

The basic operating principles of the five-phase VSI are developed as follows, assuming ideal commutation and zero forward voltage drops. The upper and lower power switches of the same leg are complimentary in operation, i.e. if the upper switch is 'ON,' the lower must be 'OFF,' and vice-versa. This is done to avoid shorting the DC supply. Complimentary operation of the switches is obtained by providing a 180-degree phase shifted gate drive signal to the two upper and lower switches.

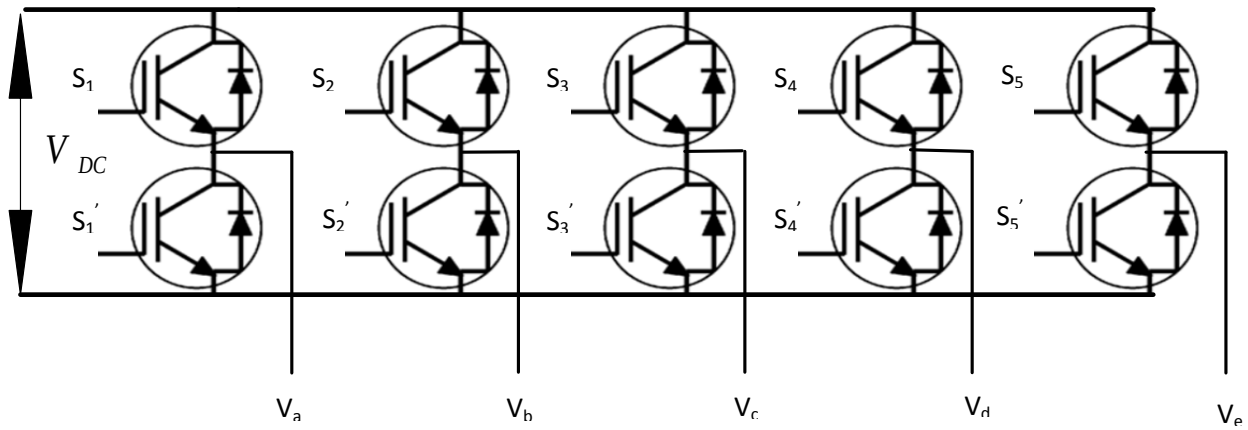


*Figure 2. 3: Power circuit topology of a five-phase voltage source inverter*

However, it is important to provide a time delay between turning 'ON' and turning 'OFF' of the two complimentary switches. This time delay is called 'Dead time,' as both the power switches remain 'OFF' simultaneously for a small duration of time. Thus the 'ON' time of each power switch is smaller compared to their corresponding 'OFF' time, which is illustrated in Figure (2.4). The upper trace shows the gate drive signal for upper switch $S_1$and the lower trace shows the gate drive signal for lower switch $S_1$. When switch $S_1$goes 'OFF,' the Switch $S_1$turns off after a delay of $t_d$ (dead time).

To simulate the dead time for inverter leg switching in MATLAB/Simulink, the block of Figure (2.2) can be used. The input to the block is the gate driving signal, where one signal is passed directly and the second signal is processed through 'Discrete Edge Detector' (from'Discrete Control blocks' of 'Extra Library' of 'Sim Power System' block-sets), then multiplied by1 (to make a complimentary signal) using a 'Gain' block. The outputs of the block of Figure (2.4). are two complimentary gate drive signals with the desired dead time. The 'Discrete Edge Detector' block is used to provide the desired dead time. This block is used when the inverter is modeled using 'Sim Power Systems block-sets,' using actual components.

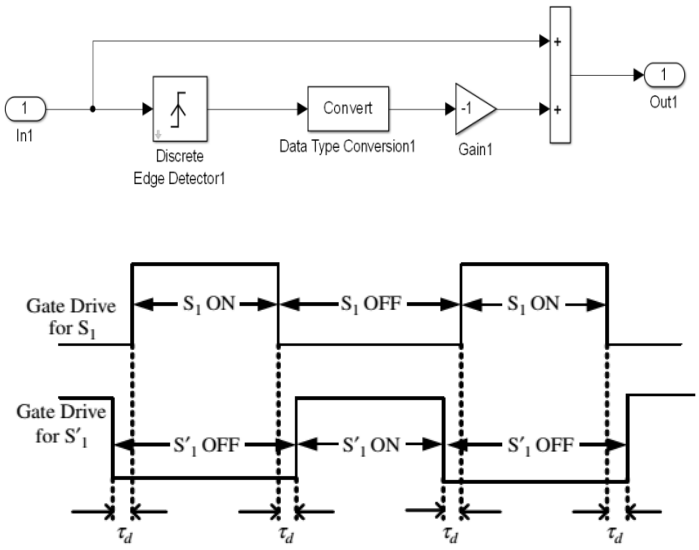


*Figure 2. 4: Illustration for dead time*

The relationship between pole voltage and switching signals is given as

$$V_k = S_k V_{dc}; k \in A, B, C, D, E \tag{2.46}$$

Where $S_k$=1 when the upper power switch is 'ON' and $S_k$=0 when the lower switch is 'ON.'

If the load is assumed to be a star connected five-phase, then the relation between the phase-to neutral load voltage and the pole voltages can be written as:

$$V_A(t) = v_a(t) + v_{nN}(t) \tag{2.47}$$

$$V_B(t) = v_b(t) + v_{nN}(t) \tag{2.48}$$

$$V_C(t) = v_c(t) + v_{nN}(t) \tag{2.49}$$

$$V_D(t) = v_d(t) + v_{nN}(t) \tag{2.50}$$

$$V_E(t) = v_e(t) + v_{nN}(t) \tag{2.51}$$

Where $V_{nN}$ is the voltage difference between the star point n of the load and the negative rail of the DC bus N, called the 'Common mode voltage'. This common mode voltage or neutral voltage is responsible of leakage bearing currents and their subsequent failure. The PWM techniques should take into account the minimization or elimination of common mode voltage. By adding each term of the equation (2.47-2.51), and putting the sum of phase-to-neutral voltage

zero (assuming a balanced five-phase voltage whose instantaneous sum is always zero), we obtain:

$$v_{nN}(t)=\frac{1}{5}\left(V_A(t)+V_B(t)+V_C(t)+V_D(t)+V_E(t)\right) \tag{2.52}$$

Substituting equation (2.47-2.51) back into equation (2.52), the following expressions for the phase-to-neutral voltage are obtained:

$$v_a(t)=\left(\frac{4}{5}\right)V_A(t)-\left(\frac{1}{5}\right)\left(V_B(t)+V_C(t)+V_D(t)+V_E(t)\right) \tag{2.53}$$

$$v_b(t)=\left(\frac{4}{5}\right)V_B(t)-\left(\frac{1}{5}\right)\left(V_A(t)+V_C(t)+V_D(t)+V_E(t)\right) \tag{2.54}$$

$$v_c(t)=\left(\frac{4}{5}\right)V_C(t)-\left(\frac{1}{5}\right)\left(V_B(t)+V_A(t)+V_D(t)+V_E(t)\right) \tag{2.55}$$

$$v_d(t)=\left(\frac{4}{5}\right)V_D(t)-\left(\frac{1}{5}\right)\left(V_B(t)+V_C(t)+V_A(t)+V_E(t)\right) \tag{2.56}$$

$$v_e(t)=\left(\frac{4}{5}\right)V_E(t)-\left(\frac{1}{5}\right)\left(V_B(t)+V_C(t)+V_D(t)+V_A(t)\right) \tag{2.57}$$

Equation (2.52-2.57) can also be written using the switching function definition of equation (2.46):

$$v_a(t)=\left(\frac{V_{dc}}{5}\right)\left[4S_A-S_B-S_C-S_D-S_E\right] \tag{2.58}$$

$$v_b(t)=\left(\frac{V_{dc}}{5}\right)\left[4S_B-S_A-S_C-S_D-S_E\right] \tag{2.59}$$

$$v_c(t)=\left(\frac{V_{dc}}{5}\right)\left[4S_C-S_A-S_B-S_D-S_E\right] \tag{2.60}$$

$$v_d(t)=\left(\frac{V_{dc}}{5}\right)\left[4S_D-S_A-S_B-S_C-S_E\right] \tag{2.61}$$

$$v_e(t)=\left(\frac{V_{dc}}{5}\right)\left[4S_E-S_A-S_B-S_C-S_D\right] \tag{2.62}$$

### 2.4.1 Ten-Step Mode of Operation

This mode of operation is an extension of the six-step operation of a three-phase voltage source inverter. The output phase voltage assumes ten different values, so is called the 'Ten-step mode.' The switching frequency of the power switches in this mode is equal to the fundamental output voltage frequency. Each power switch operates for half of the fundamental cycle and so is called the 180-degree conduction mode. Thus each power switch turns 'ON' and turns 'OFF' only once in the whole fundamental cycle. The output in maximum in this mode and switching losses are minimal. However, the output in mode contains a considerable amount of low-order harmonics, which decreases the performance of the load. The upper power switch is 'ON' when the load current is positive (current flowing from inverter to the load) and the pole voltage is positive, and the anti-parallel diode across the upper switch is turned 'ON' when the load current is negative while the pole voltage is also positive. The lower power switch is turned 'ON' when the load current is positive and the pole voltage is zero or negative (depending upon the choice of DC link, i.e. $+V_{dc}$ and 0 or $+0.5V_{dc}$ and $-0.5V_{dc}$) and the lower anti-parallel diode is turned on for a negative load current. The possible pole voltages during the step operation of the five-phase VSI and the corresponding switches that are 'ON' are listed in Table (2.2).

The switching signal for the ten-step mode of operation is given in Figure (2.5). The delay in switching between the two consecutive phases are 360/5=72. The complementary gate drive signals are also shown.

| Mode | Switches ON | $V_A$ | $V_B$ | $V_C$ | $V_D$ | $V_E$ |
|---|---|---|---|---|---|---|
| **1** | $S_1,S_2,S'_3,S'_4,S_5$ | $V_{dc}$ | $V_{dc}$ | **0** | **0** | $V_{dc}$ |
| **2** | $S_1,S_2,S'_3,S'_4,S'_5$ | $V_{dc}$ | $V_{dc}$ | **0** | **0** | **0** |
| **3** | $S_1,S_2,S_3,S'_4,S'_5$ | $V_{dc}$ | $V_{dc}$ | $V_{dc}$ | **0** | **0** |
| **4** | $S'_1,S_2,S_3,S'_4,S'_5$ | **0** | $V_{dc}$ | $V_{dc}$ | **0** | **0** |
| **5** | $S'_1,S_2,S_3,S_4,S'_5$ | **0** | $V_{dc}$ | $V_{dc}$ | $V_{dc}$ | **0** |
| **6** | $S'_1,S'_2,S_3,S_4,S'_5$ | **0** | **0** | $V_{dc}$ | $V_{dc}$ | **0** |
| **7** | $S'_1,S'_2,S_3,S_4,S_5$ | **0** | **0** | $V_{dc}$ | $V_{dc}$ | $V_{dc}$ |
| **8** | $S'_1,S'_2,S'_3,S_4,S_5$ | **0** | **0** | **0** | $V_{dc}$ | $V_{dc}$ |
| **9** | $S_1,S'_2,S'_3,S_4,S_5$ | $V_{dc}$ | **0** | **0** | $V_{dc}$ | $V_{dc}$ |
| **10** | $S_1,S'_2,S'_3,S'_4,S_5$ | $V_{dc}$ | **0** | **0** | **0** | $V_{dc}$ |

*Table 2. 2: Pole voltages of the five-phase VSI during step mode of operation*

For a star connected load. It is evident that the phase-to-neutral voltage takes on four different values/levels and ten steps in one fundamental cycle.In a five-phase system, there exist two different systems of line voltages, termed 'Adjacent line-to-line voltage' and 'Non-adjacent line-to-line voltage,' as illustrated in Figure (). The phase voltages are represented as ($v_a$,$v_b$,$v_c$,$v_d$,$v_e$) the adjacent line voltages are denoted as ($v_{ab}$,$v_{bc}$,$v_{cd}$,$v_{de}$,$v_{ea}$) and the non-adjacent line voltages are given as ($v_{ac}$,$v_{bd}$,$v_{ce}$,$v_{da}$,$v_{eb}$) The relationship between the adjacent, non-adjacent, and phase voltages are elaborated upon by using a numerical example.

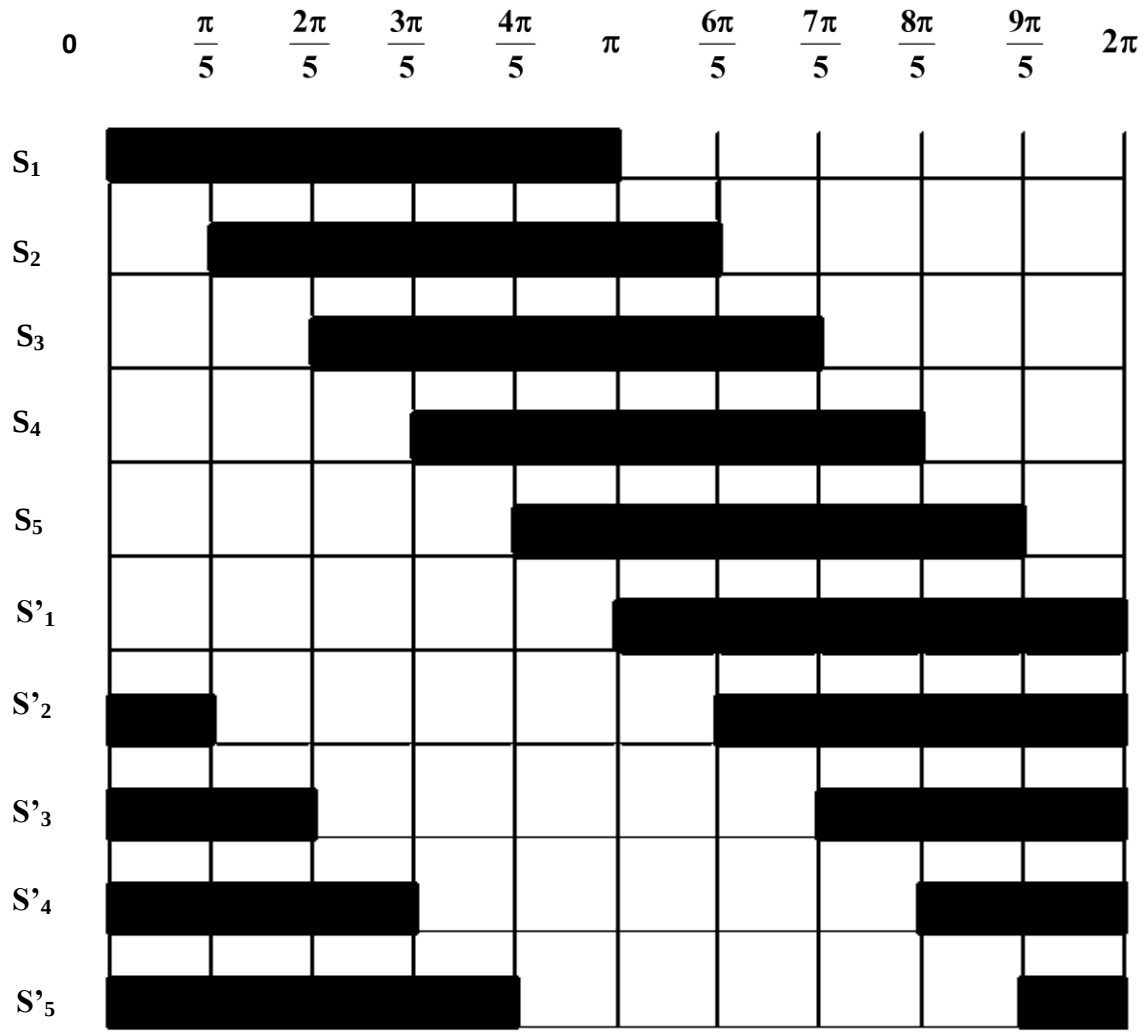


*Figure 2. 5 Gate drive signal for a ten-step mode of operation*

| Mode | Switches ON | $V_a$ | $V_b$ | $V_c$ | $V_d$ | $V_e$ |
|---|---|---|---|---|---|---|
| **1** | $S_1,S_2,S'_3,S'_4,S_5$ | $2/5\ V_{dc}$ | $2/5\ V_{dc}$ | $-3/5\ V_{dc}$ | $-3/5\ V_{dc}$ | $2/5\ V_{dc}$ |
| **2** | $S_1,S_2,S'_3,S'_4,S'_5$ | $3/5\ V_{dc}$ | $3/5\ V_{dc}$ | $-2/5\ V_{dc}$ | $-2/5\ V_{dc}$ | $-2/5\ V_{dc}$ |
| **3** | $S_1,S_2,S_3,S'_4,S'_5$ | $2/5\ V_{dc}$ | $2/5\ V_{dc}$ | $2/5\ V_{dc}$ | $-3/5\ V_{dc}$ | $-3/5\ V_{dc}$ |
| **4** | $S'_1,S_2,S_3,S'_4,S'_5$ | $-2/5\ V_{dc}$ | $3/5\ V_{dc}$ | $3/5\ V_{dc}$ | $-2/5\ V_{dc}$ | $-2/5\ V_{dc}$ |
| **5** | $S'_1,S_2,S_3,S_4,S'_5$ | $-3/5\ V_{dc}$ | $2/5\ V_{dc}$ | $2/5\ V_{dc}$ | $2/5\ V_{dc}$ | $-3/5\ V_{dc}$ |
| **6** | $S'_1,S'_2,S_3,S_4,S'_5$ | $-2/5\ V_{dc}$ | $-2/5\ V_{dc}$ | $3/5\ V_{dc}$ | $3/5\ V_{dc}$ | $-2/5\ V_{dc}$ |
| **7** | $S'_1,S'_2,S_3,S_4,S_5$ | $-3/5\ V_{dc}$ | $-3/5\ V_{dc}$ | $2/5\ V_{dc}$ | $2/5\ V_{dc}$ | $2/5\ V_{dc}$ |
| **8** | $S'_1,S'_2,S'_3,S_4,S_5$ | $-2/5\ V_{dc}$ | $-2/5\ V_{dc}$ | $-2/5\ V_{dc}$ | $3/5\ V_{dc}$ | $3/5\ V_{dc}$ |
| **9** | $S_1,S'_2,S'_3,S_4,S_5$ | $2/5\ V_{dc}$ | $-3/5\ V_{dc}$ | $-3/5\ V_{dc}$ | $2/5\ V_{dc}$ | $2/5\ V_{dc}$ |
| **10** | $S_1,S'_2,S'_3,S'_4,S_5$ | $3/5\ V_{dc}$ | $-2/5\ V_{dc}$ | $-2/5\ V_{dc}$ | $-2/5\ V_{dc}$ | $3/5\ V_{dc}$ |

*Table 2. 3 Phase-to-neutral voltages of a star connected load supplied from a five-phase VSI*

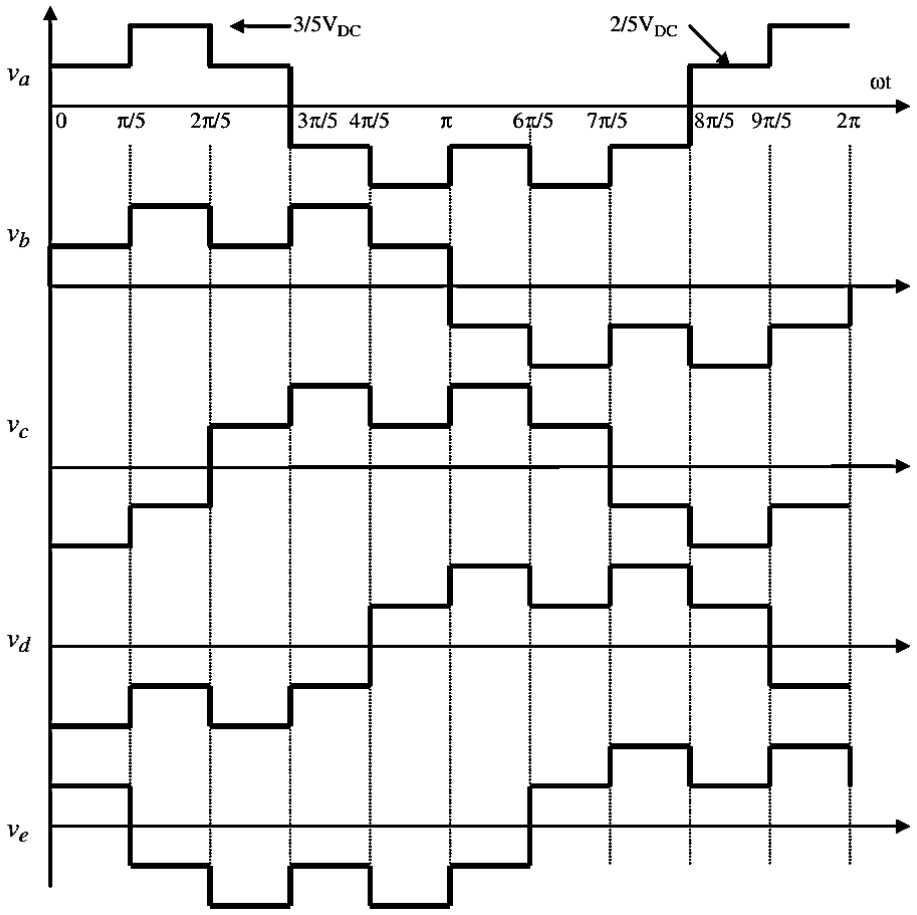


*Figure 2. 6 Phase-to-neutral voltage of a five-phase VSI in ten-step mode*

| Mode | Switches ON | $V_{ab}$ | $V_{bc}$ | $V_{cd}$ | $V_{de}$ | $V_{ea}$ |
|---|---|---|---|---|---|---|
| **1** | $S_1,S_2,S'_3,S'_4,S_5$ | **0** | $V_{dc}$ | **0** | $-V_{dc}$ | **0** |
| **2** | $S_1,S_2,S'_3,S'_4,S'_5$ | **0** | $V_{dc}$ | **0** | **0** | $-V_{dc}$ |
| **3** | $S_1,S_2,S_3,S'_4,S'_5$ | **0** | **0** | $V_{dc}$ | **0** | $-V_{dc}$ |
| **4** | $S'_1,S_2,S_3,S'_4,S'_5$ | $-V_{dc}$ | **0** | $V_{dc}$ | **0** | **0** |
| **5** | $S'_1,S_2,S_3,S_4,S'_5$ | $-V_{dc}$ | **0** | **0** | $V_{dc}$ | **0** |
| **6** | $S'_1,S'_2,S_3,S_4,S'_5$ | **0** | $-V_{dc}$ | **0** | $V_{dc}$ | **0** |
| **7** | $S'_1,S'_2,S_3,S_4,S_5$ | **0** | $-V_{dc}$ | **0** | **0** | $V_{dc}$ |
| **8** | $S'_1,S'_2,S'_3,S_4,S_5$ | **0** | **0** | $-V_{dc}$ | **0** | $V_{dc}$ |
| **9** | $S_1,S'_2,S'_3,S_4,S_5$ | $V_{dc}$ | **0** | $-V_{dc}$ | **0** | **0** |
| **10** | $S_1,S'_2,S'_3,S'_4,S_5$ | $V_{dc}$ | **0** | **0** | $-V_{dc}$ | **0** |

*Table 2. 4: Adjacent line-to-line voltages of the five-phase VSI*

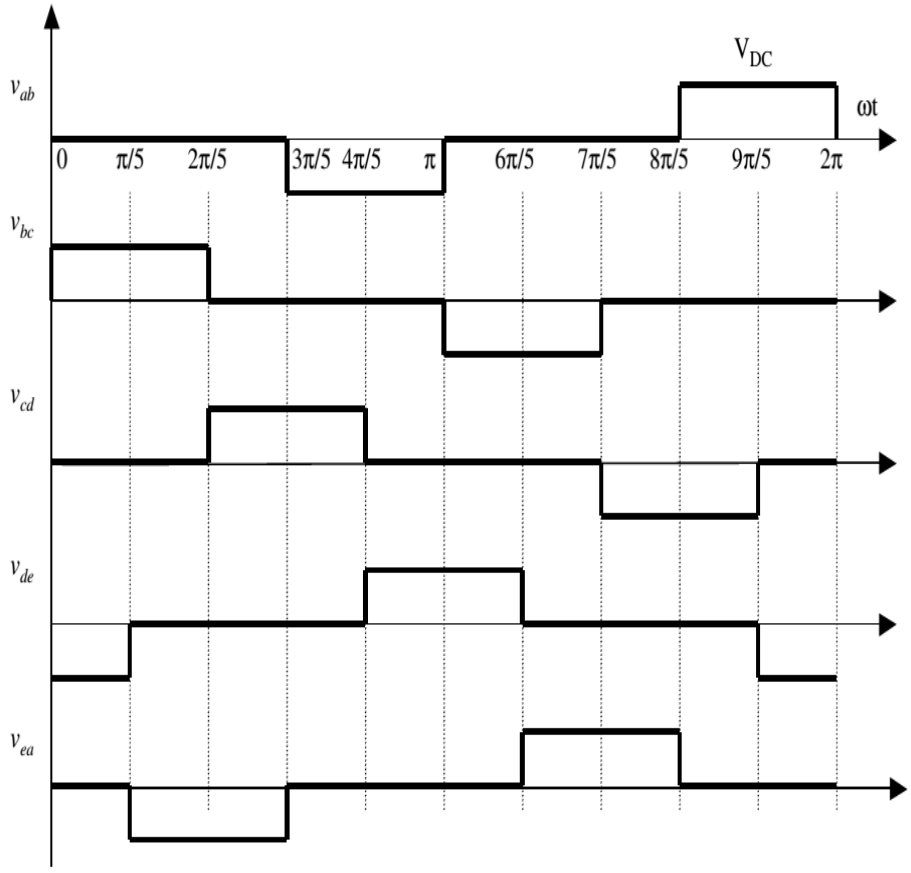


*Figure 2. 7: adjacent line-to-line voltages of the five-phase VSI*

| Mode | Switches ON | $V_{ab}$ | $V_{bc}$ | $V_{cd}$ | $V_{de}$ | $V_{ea}$ |
|---|---|---|---|---|---|---|
| **1** | $S_1,S_2,S'_3,S'_4,S_5$ | $V_{dc}$ | $V_{dc}$ | $-V_{dc}$ | $-V_{dc}$ | **0** |
| **2** | $S_1,S_2,S'_3,S'_4,S'_5$ | $V_{dc}$ | $V_{dc}$ | **0** | $-V_{dc}$ | $-V_{dc}$ |
| **3** | $S_1,S_2,S_3,S'_4,S'_5$ | **0** | $V_{dc}$ | $V_{dc}$ | $-V_{dc}$ | $-V_{dc}$ |
| **4** | $S'_1,S_2,S_3,S'_4,S'_5$ | $-V_{dc}$ | $V_{dc}$ | $V_{dc}$ | **0** | $-V_{dc}$ |
| **5** | $S'_1,S_2,S_3,S_4,S'_5$ | $-V_{dc}$ | **0** | $V_{dc}$ | $V_{dc}$ | $-V_{dc}$ |
| **6** | $S'_1,S'_2,S_3,S_4,S'_5$ | $-V_{dc}$ | $-V_{dc}$ | $V_{dc}$ | $V_{dc}$ | **0** |
| **7** | $S'_1,S'_2,S_3,S_4,S_5$ | $-V_{dc}$ | $-V_{dc}$ | **0** | $V_{dc}$ | $V_{dc}$ |
| **8** | $S'_1,S'_2,S'_3,S_4,S_5$ | **0** | $-V_{dc}$ | $-V_{dc}$ | $V_{dc}$ | $V_{dc}$ |
| **9** | $S_1,S'_2,S'_3,S_4,S_5$ | $V_{dc}$ | $-V_{dc}$ | $-V_{dc}$ | **0** | $V_{dc}$ |
| **10** | $S_1,S'_2,S'_3,S'_4,S_5$ | $V_{dc}$ | **0** | $-V_{dc}$ | $-V_{dc}$ | $V_{dc}$ |

*Table 2. 5:non-adjacent line-to-line voltages of the five-phase VSI*

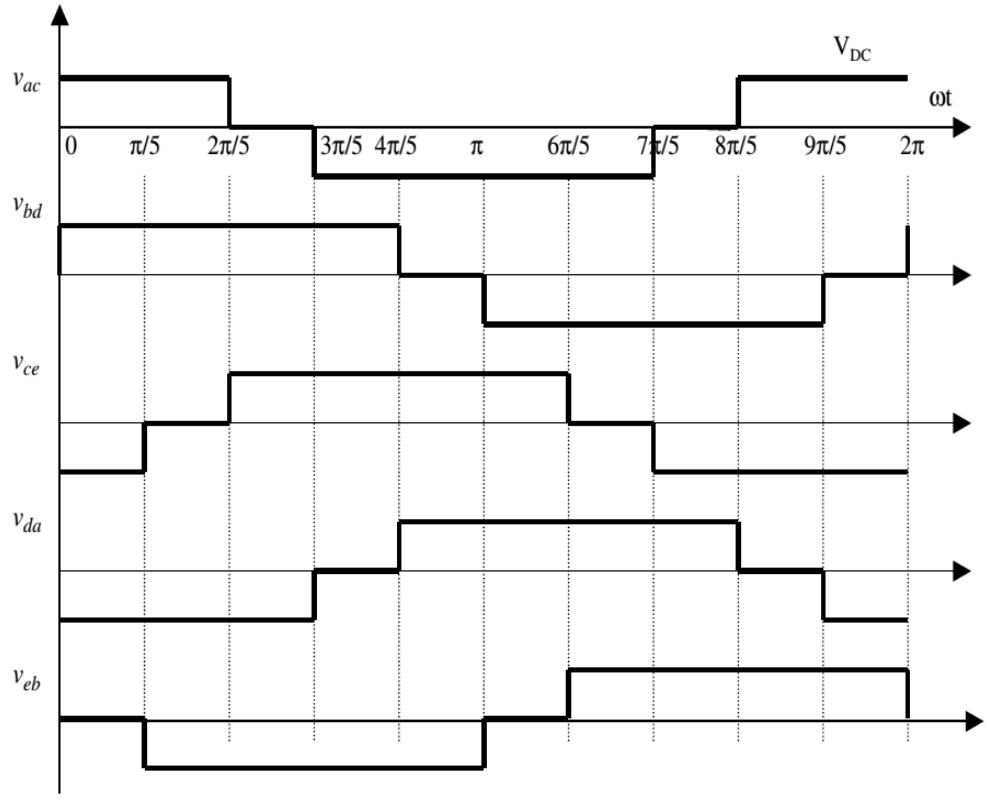


Figure 2. 8: *Non-adjacent line-to-line voltages of the five-phase VSI*

### 2.4.2 Fourier analysis of the five-phase inverter output voltages

In order to relate the input dc link voltage of the inverter with the output phase-to-neutral and line-to-line voltages, Fourier analysis of the voltage waveforms is undertaken in this section. Out of the two sets of the line-to-line voltages, discussed in the preceding subsection, only non-adjacent line-to-line voltages are analyzed since they have higher fundamental harmonic values than the adjacent line-to-line voltages.

Using definition of the Fourier series for a periodic waveform:

$$v(t) = V_0 + \sum \left( A_k \cos k\omega t + B_k \sin k\omega t \right) \tag{2.63}$$

Where the coefficients of the Fourier series are given by

$$V_0 = \frac{1}{T}\int v(t)dt = \frac{1}{2\pi}\int v(\theta)d\theta \tag{2.64}$$

$$A_k = \frac{2}{T}\int v(t)\cos k\omega t dt = \frac{1}{\pi}\int v(\theta)\cos k\theta d\theta \tag{2.65}$$

$$B_k = \frac{2}{T}\int v(t)\sin k\omega t dt = \frac{1}{\pi}\int v(\theta)\sin k\theta d\theta \tag{2.66}$$

and observing that the waveforms possess quarter-wave symmetry and can be conveniently taken as odd functions, we can represent phase-to-neutral voltages and line-to-line voltages with the following expressions:

$$v(t) = \sum_{k=0}^{\infty} B_{2k+1} \sin(2k+1)\omega t = \sqrt{2}\sum_{k=0}^{\infty} V_{2k+1} \sin(2k+1)\omega t \tag{2.67}$$

$$B_{2k+1} = \sqrt{2}V_{2k+1} = \frac{4}{\pi}\int_0^{\pi/2} v(\theta)\sin(2k+1)\theta d\theta \tag{2.68}$$

In the case of the phase-to-neutral voltage $V_b$, shown in Figure (), the coefficients of the

Fourier series are:

$$B_{2k+1} = \frac{4}{5\pi}V_{DC}\frac{1}{2k+1}\left[2 + \frac{\pi}{5}\cos(2k+1) - \frac{2\pi}{5}\cos(2k+1)\right] \tag{2.69}$$

The expression in brackets in the second equation () equals zero for all harmonics whose order is divisible by five. For all the other harmonics, it equals 2.5. Hence, we can write the Fourier series of the phase-to-neutral voltage as:

$$v(t)=\frac{2}{\pi}V_{DC}\left[\sin\omega t+\frac{1}{3}\sin 3\omega t+\frac{1}{7}\sin 7\omega t+\frac{1}{9}\sin 9\omega t+...\right] \tag{2.70}$$

From equation (2.70) it follows that the fundamental component of the output phase-to neutral voltage has an rms value of

$$V_1=\frac{\sqrt{2}}{\pi}V_{DC}=0.45V_{DC} \tag{2.71}$$

It is observed that the fundamental output of a five-phase voltage source inverter is the same as that of a three-phase voltage source inverter. Fourier analysis of the non-adjacent line-to-line voltages is performed in the same manner. Fourier series remains to be given by equation (2.70). Taking the second voltage in Figure (2.71) and shifting the zero time instant by pi/10 degrees to the left, we have the following Fourier series coefficients:

$$B_{2k+1}=\frac{4}{\pi}\int_{\pi/10}^{\pi/2}V_{DC}\sin(2k+1)\theta d\theta=\frac{4}{\pi}V_{DC}\frac{1}{2k+1}\cos(2k+1)\frac{\pi}{10} \tag{2.72}$$

Hence the Fourier series of the non-adjacent line-to-line voltage is

$$v(t)=\frac{4}{\pi}V_{DC}\left[0.95\sin\omega t+\frac{0.59}{3}\sin 3\omega t-\frac{0.59}{7}\sin 7\omega t-\frac{0.95}{9}\sin 9\omega t-...\right] \tag{2.73}$$

and the fundamental harmonic rms value of the non-adjacent line-to-line voltage is

$$V_{1L}=\frac{2\sqrt{2}}{\pi}V_{DC}\cos\frac{\pi}{10}=0.856V_{DC}=1.902V_1 \tag{2.74}$$

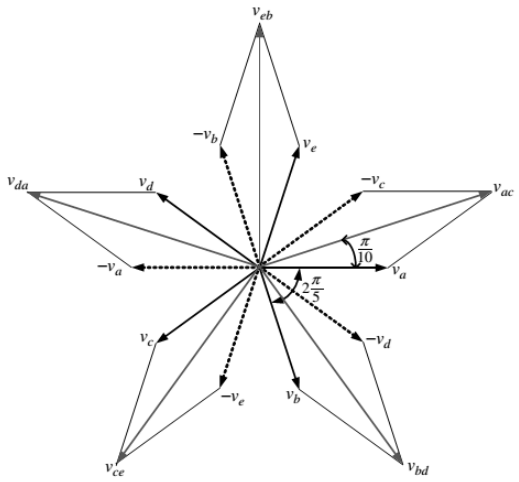


*Figure 2. 9: Phase and adjacent line voltage concept*

## 2.4 Literature review

Literature review of some of the relevant research in the areas of multi-phase machines has been detailed in ***Jones (2002) and Jones (2005)***. The various aspects covered have included advantages of multi-phase machines over their three phase counterparts, modelling and control of multi-phase machines, three-phase multi-motor drives, etc. This chapter reviews the latest progress made in the area of multi-phase machine drives, highlighting several other relevant aspects and addressing the features of the drives not covered in ***Jones (2002) and Jones (2005)***. Although the references are available for drive phase numbers equal to five, six, seven, nine and even fifteen, the literature review focuses on five-phase drives. The chapter gives an overview of the following aspects relevant for the project: application areas of multi-phase machines, the techniques for reduction of the switch power rating and count in three-phase motor drives supplied from three-phase inverters, and the modelling and control of multi-phase and three-phase inverters. It additionally includes a review of the newest developments in five-phase motor drives, with an emphasis on papers published from 2002 onwards and not covered by ***Jones (2002) and Jones (2005).***

### 2.4.1 five-phase motor drives

Direct torque control (DTC) is one of the powerful methods for high performance control of motor drives, which has become an industrially accepted standard for three-phase induction machines. The basic operating principle of DTC is based on instantaneous space vector theory and relies on utilization of the non-ideal inverter nature to achieve good dynamic control. ***Toliyat***

***and Xu (2000)*** have recently extended the DTC concept to a five phase induction motor control and they presented a comparison between the three-phase and five-phase DTC drives. The implementation of the control system was done using 32 bit floating point TMS320C32 DSP. The three-phase inverter has only eight voltage space vectors that can be applied to a motor, while a five-phase inverter has 32 possible voltage space vectors. There is therefore a greater flexibility in controlling a five-phase drive system. The authors achieved high performance in terms of precise and fast flux and torque control and a smaller torque and flux ripple for five-phase induction machine as compared to three phase induction machine.

Vector control and direct torque control of a five-phase induction motor with concentrated full-pitch winding was also developed and implemented again using 32 bit floating point DSP TMS320C32 in ***Xu et al (2002a)***. The proposed vector controller uses fundamental current in conjunction with 15% third harmonic stator current injection to provide quasi-rectangular current, which yields rectangular air gap flux in the concentrated winding induction motor. It was shown that this approach enhances torque output by 11.2% under dynamic condition and by 10% during steady state operation, compared to the case when only fundamental current is fed to the machine. The DTC provides high performance in terms of smaller current, flux and torque ripples due to large number of space vectors for controlling the machine. Further, zero switching vectors are not needed to implement space vector modulation for five-phase PWM inverter for DTC and thus the wear and tear of motor bearing can be avoided. ***Shi and Toliyat (2002***) have developed the vector control scheme based on space vector PMW for a five-phase synchronous reluctance motor drive. The control system for the proposed drive was again implemented using 32 bit floating point DSP TMS320C32.

A special current control scheme has been developed for a five-phase induction motor drive by ***Xu et al (2002b)***, which enables operation under open-circuit fault condition with loss of one or two phases. Concentrated winding induction motor was considered for the study and thus third harmonic current was used in conjunction with the fundamental component to obtain rectangular air–gap flux profile. The amplitudes of the fundamental and the third harmonic current need proper adjustment under fault condition. The speed and load have to be lowered under loss of two phases in order to prevent the stator current from exceeding the rated value. The whole system was implemented to validate the theoretical findings.

A detailed performance analysis of concentrated winding multi-phase induction motors encompassing multiple of three and non-multiple of three numbers of phases was carried out by ***Toliyat and Qahtany (2002)*** using finite element analysis (FEA) method. The study reveals the fact that the torque pulsation decreases with an increase in the number of phases due to smaller step changes in MMF, except in seven-phase case where ripple was high due to cogging phenomena. The efficiency was seen to improve with increasing number of phases because of the reduction in ripple in rotor current. Further the five-phase machine was seen to provide the highest torque to current ratio due to an increase in the amplitude of fundamental MMF. The FEA results also showed a decrease in the stator back iron flux and an increase in stator tooth flux if third harmonic current is injected along with the fundamental in the five-phase induction motor. This suggests a new geometry (pancake shape) for a five phase machine stator supplied by the third harmonic along with the fundamental. A comparison of performance was also given for different multi-phase machines with respect to the conventional three-phase distributed winding induction motor.

A general modelling approach encompassing dynamic and control issues for a five phase permanent magnet brushless dc machine was presented by ***Franceschetti and Simoes (2001)***. The simulation was done for a five-phase, twelve-pole machine with rated torque of 30 Nm, with concentrated stator winding. The same machine type, which requires square wave current for its normal operation, has been considered in ***Simoes et al (2001)*** as well, where experimental implementation was based on Motorola 56824 DSP. The switching frequency of the inverter was set to 10 kHz. Five-phase trapezoidal back-emf permanent magnet synchronous machine was elaborated by ***McCleer et al (1991)*** as well. The motor was supplied from a five-phase VSI in $144^{o}$ conduction mode with square wave currents. The five phase machine was shown to have higher torque capacity compared to similar sized three phase machine and lower peak VA requirement of the switching devices.

The modelling and analysis of a five-phase permanent magnet synchronous machine supplied from a five-phase PWM inverter under normal and fault conditions (one phase open circuited) was examined by ***Robert-Dehault et al (2002)***. The linear permanent magnet machine model was developed in phase variable form for fault condition and also its d-q form was given for normal operating conditions. The machine leakage reactance was considered as 5% with PWM inverter

commutating at 2 kHz. The proposed control strategy allows the machine to produce the same torque under fault condition as under normal condition, with very small torque ripple (6% torque ripple was observed because of the current controller type). ***Pereira and Canalli (2002)*** have presented the design, modelling and performance analysis of a five-phase permanent magnet synchronous machine operating as a generator feeding a resistive load through five-phase bridge rectifier. The parameters of the machine were determined using FEA. The performance in terms of load voltage versus current, output power, rectified voltage waveform, phase to neutral and phase to phase voltages and phase currents of the machine was assessed and examined using simulation and actual measurements.

### 2.4.2 Control of multi-phase voltage source inverters

The use of multi-phase inverter was first reported by ***Ward and Härer (1969)*** in a variable speed five-phase induction motor drive application. It utilized a forced commutated thyristor based inverter in ten-step operating mode. The torque ripple was decreased to one third compared to the equivalent three-phase case and was at an increased frequency. However, the machine current contained strong third harmonic component, which generated additional losses. To avoid these losses and to obtain fast current control, several PWM techniques for multi-phase VSIs have been developed, such as those reported in ***Pavitharan et al (1988), Toliyat (1998) and Toliyat et al (2000).***

A complete mathematical model of a five-phase VSI, based on space vector representation, was developed by ***Toliyat et al (1993)***. The inverter operation in ten-step mode and PWM mode was discussed. The hysteresis type PWM current regulation was used for the drive under rotor flux oriented indirect vector control conditions. A SVPWM was proposed by ***Gataric (2000)*** for a five-phase VSI control in conjunction with induction motor drives. The same strategy was employed by Shi and ***Toliyat (2002) and Toliyat et al (2000)*** in a five phase synchronous reluctance motor drive. ***Gopakumar et al (1993)*** employed SVPWM technique in split-phase induction motor drive fed by six-phase VSI.

***Takami and Matsumoto (1993)*** have proposed optimum pulse pattern PWM for large capacity nine-phase VSI feeding a nine-phase induction motor (with three sets of three-phase windings on the stator with isolated neutral points and a single three-phase winding on the rotor). The current control loop was eliminated from the inverter control system. A new configuration, which

includes nine low-rating (20% of the motor capacity) single-phase reactors, was introduced. The reactor turns ratio was selected equal to 1:2 sin(π/18):1 so as to eliminate the lower order harmonics (5th, 7th, $11^{th}$ and 13th) from the inverter/motor phase voltages and currents and also to balance the fundamental currents in the event of unbalancing. To eliminate even harmonics from the current/voltage waveform the optimal pulse pattern was developed based on Lagrangian multiplier method. The proposed optimal pulse pattern PWM technique was compared with the ramp-comparison PWM and it was shown to reduce the harmonic amplitudes to a significantly lower value. The proposed configuration also reduces the electromagnetic noise of the motor to a great extent.

***Kelly et al (2001)*** have examined general n-phase (leg) inverter control techniques taking nine-phase inverter as a specific example. Ann-phase inverter has (n-1)/2 possible load equivalent circuits and each operates in n-step mode to produce a unique step voltage waveform with different fundamental and harmonic contents. The nine-phase inverter was examined for four different load equivalent configurations in eighteen-step mode and 4-5 configuration was found to be the optimum choice because of the highest switching efficiency (only one switch changes state between conduction intervals), maximum phase current delivery and maximum fundamental content. Four different SVPWM techniques have been developed for the general n-phase inverter. The first technique is a natural extension of the conventional three-phase SVPWM and it resulted in lower dc bus utilization. The second technique asks for injection of √n order harmonic, resulting in higher dc bus utilization (maximum attainable fundamental component increases). However, √n separate neutrals have to be used. The third proposed technique utilizes smaller number of space vectors (74 instead of 512) but the switching efficiency was found to be poor in this case (in the case of nine phase inverter, eighteen switches change state between conduction intervals). To improve the switching efficiency the fourth technique was proposed, which does not use zero space vectors (in the case of a nine-phase inverter, only six switches change state between conduction intervals). The first proposed technique (SVPWM) in the above referenced work was compared analytically and by experimentation to the ramp-comparison PWM by ***Kelly et al (2003)*** in conjunction with a nine-phase inverter fed nine-phase induction motor drive. The SVPWM was shown to enhance the fundamental by 1.55% compared to the sine-triangle PWM and thus enables better utilization of the dc bus.

# CHAPTER THREE

## METHODOLOGY

### 3.1 Introduction

The control strategy of the drive system which has three distinct parts: the v-f control, the stator resistance voltage compensation and the slip frequency compensation. A strategic block diagram of closed loop speed control is shown in Figure 3.1.The actual speed of the secondary member $\omega_m$ is compared with its commanded value $\omega^*$ and the error is processed through a PI controller and a limiter to obtain the slip-speed command $\omega_{sl}$.The limiter ensures that the slip speed command is within the maximum allowable slip speed of the $L_{IM}$. The slip speed command is added to the speed of the secondary member to obtain the synchronous speed, $\omega_s$ for generating a frequency command. This frequency command is next multiplied by the number of pole pairs (PP) to obtain the reference output frequency, $\omega^*$ of the inverter. The frequency command then generates a voltage command through a volts/Hz function generator. To compensate for the primary-member-resistance-voltage drop, a boost voltage is added to the generated voltage so that the desired rated flux and hence the corresponding thrust becomes available down to zero speed. Effect of boost voltage, however, becomes negligible at higher frequencies.

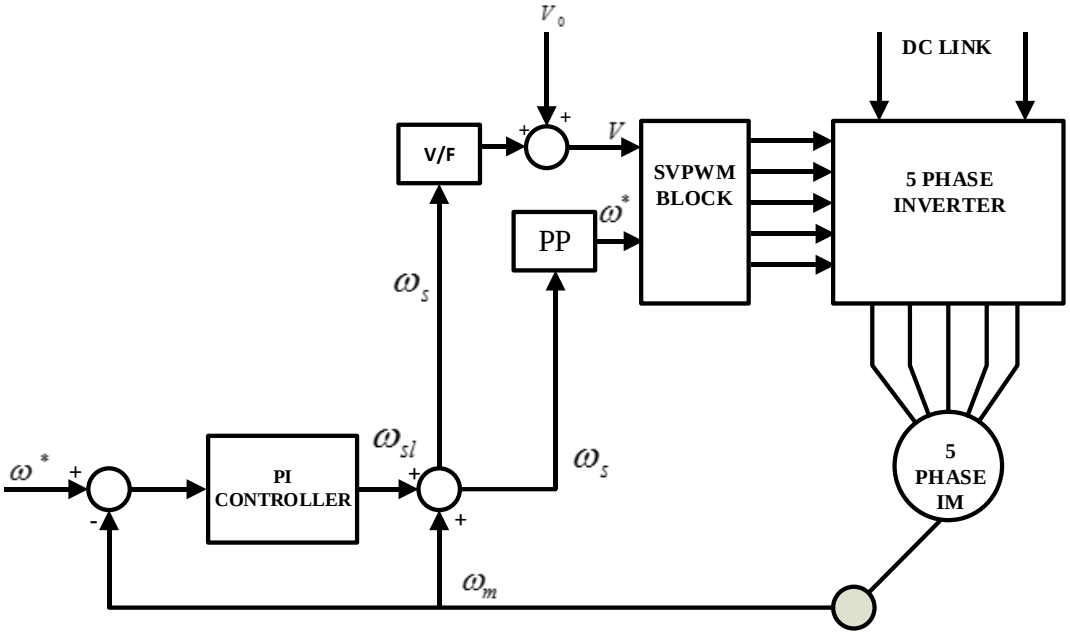


*Figure 3. 1 Constant V/F control scheme for a five phase drive*

## 3.2 V/F Control Scheme

Induction motors employ a simple but clever scheme of electromechanical energy conversion. In the squirrel-cage motors, which constitute a vast majority of induction machines, the rotor is inaccessible. No moving contacts, such as the commutator and brushes in dc machines or slip rings and brushes in ac synchronous motors and generators, are needed. This arrangement greatly increases reliability of induction motors and eliminates the danger of sparking, permitting squirrel-cage machines to be safely used in harsh environments, even in an explosive atmosphere. An additional degree of ruggedness is provided by the lack of wiring in the rotor, whose winding consists of un insulated metal bars forming the squirrel cage that gives the name to the motor. Such a robust rotor can run at high speeds and withstand heavy mechanical and electrical overloads. In adjustable-speed drives (ASDs), the low electric time constant speeds up the dynamic response to control commands. Typically, induction motors have a significant torque reserve and a low dependence of speed on the load torque. There are various methods for the speed control of an Induction Motor. They are: Pole Changing, Variable Supply Frequency Control, Variable Supply Voltage Control, Variable Rotor Resistance Control,V/f Control, Slip Recovery and Vector Control.

Of the above mentioned methods, V/f Control is the most popular and has found widespread use in industrial and domestic applications because of its ease-of-implementation. However, it has inferior dynamic performance compared to vector control. Thus in areas where precision is required, V/f Control are not used. The various advantages of V/f Control are as follows:

i. It provides good range of speed.

ii. It gives good running and transient performance.

iii. It has low starting current requirement.

iv. It has a wider stable operating region.

v. Voltage and frequencies reach rated values at base speed.

vi. The acceleration can be controlled by controlling the rate of change of supply frequency.

vii. It is cheap and easy to implement.

In the V/Hz control, the speed of induction motor is controlled by the adjustable magnitude of stator voltages and frequency in such a way that the air gap flux is always maintained at the

desired value at the steady-state. Sometimes this scheme is called the scalar control because it focuses only on the steady state dynamic. It can explain how this technique works by looking at the simplified version of the steady state equivalent circuit as seen in Figure 3. According to in this figure, the stator resistance ($R_s$) is assumed to be zero and the stator leakage inductance ($L_{ls}$) is embedded into the (referred to stator) rotor Leakage inductance ($L_{lr}$) and the magnetizing inductance, which is representing the amount of air gap flux, is moved in front of the total leakage inductance ($L_l = L_{ls} + L_{lr}$). As a result, the magnetizing current that generates the air gap flux can be approximately the stator voltage to frequency ratio.

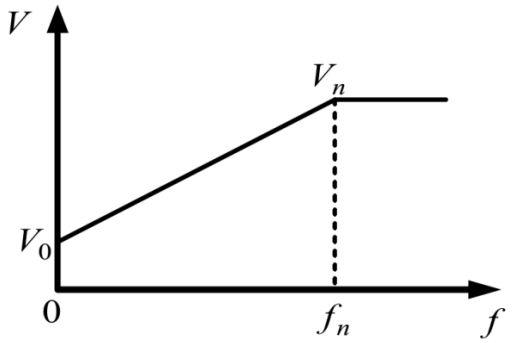


*Figure 3. 2 v/f profile*

Assuming that the voltage drop across the stator resistance is small in comparison with the stator voltage, the stator flux can be expressed as

$$\Lambda_S = \frac{V_s}{\omega} = \frac{1}{2\pi}\left(\frac{V_s}{f}\right) \tag{3.1}$$

Where, $\Lambda_S$ is flux linkage and $\omega$ is the angular velocity of the motor.

## 3.3 Space Vector Pulse Width Modulation (SVPWM) Technique

SVPWM has become one of the most popular PWM techniques, because of its easier digital implementation and better DC bus utilization, when compared to the carrier-based sinusoidal PWM method. The principle of SVPWM lies in the switching of the inverter in a special way, so as to apply a set of space vectors for a specific time. As seen in the previous section, a five-phase VSI yields 32 space vectors spanning over 360 degrees, forming a decagon with 10 sectors of 36 degrees each. The reference voltage is synthesized by switching between the neighboring vectors, such that the volt-second balance is maintained. Two neighboring active vectors are

employed to implement SVPWM, thus as an extension in a five-phase VSI, also two neighboring active space vector can be used. However, the next section shows that simple extension of SVPWM leads to distortion in the output voltage. Hence, it is realized that instead of two, four neighboring vectors when used to implement SVPWM will lead to sinusoidal output voltages. As a rule of thumb=n-1(n phase number) numbers of active space vectors are needed to generate sinusoidal output in multi-phase voltage source inverter [4].

Thus there exists more than one method of implementing SVPWM in a multi-phase voltage source inverter. Nevertheless, an ideal SVPWM of a five-phase inverter should satisfy a number of requirements. First, in order to keep the switching frequency constant, each switch can change state only twice in the switching-period (once 'ON' to 'OFF' and once 'OFF' to 'ON', or vice-versa). Second, the rms value of the fundamental phase voltage of the output must equal the rms of the reference space vector. Third, the scheme must provide full utilization of the available DC bus voltage [5]. Finally, since the inverter is aimed at supplying the load with sinusoidal voltages, the low-order harmonic content needs to be minimized (this especially applies to the 3rd and 7th harmonics). These criteria are used in assessing the merits and demerits of various SVPWMs. Two methods are elaborated here, one with two active space vectors and one with four active vectors.

Two neighboring active space vectors and two zero space vectors are used in one switching period to synthesize the input reference voltage. There are five legs in a five-phase inverter, each with two power switches whose operations are complimentary. In one switching period, each power switch will change its state twice (from 'OFF' to 'ON' and then from 'ON' to 'OFF'), hence in total, ten switching's take place in one switching period. The switching patterns are pre-formulated and stored in a look-up table. The switching is done in such a way that in the first switching half-period, the first zero vector is applied, followed by two active state vectors and then by the second zero state vector. The second switching half-period is the mirror image of the first. The symmetrical SVPWM is achieved in this way. This method is the simplest extension of space vector modulation of three-phase VSIs.

When using two large length and two medium length active vectors, their mapping in the x-y plane is such that they cancel each other, as illustrated in Figure.3.4 for sector I and it follows for the rest of the sectors. Since vector numbers 16 and 25 are opposite to each other, and so are 24

and 29, their lengths are different (ratio of lengths of larger to smaller be 1.618). Thus if the time of application of the smaller vector is increased in the same proportion, they will have equal volt-second and will cancel each other, eliminating the x-y components and generating sinusoidal output.

Since a five-phase system is under consideration, the vector needs to be analyzed in a five dimensional space. Decoupling transformation leads to two orthogonal planes, namely d-q, x-y and a zero sequence component. The space vectors in the two orthogonal planes are defined as

$$\underline{v}_{\alpha-\beta} = \frac{2}{5}\left(v_a + \underline{a}v_b + \underline{a}^2 v_c + \underline{a}^4 v_d + \underline{a}^6 v_e\right) \tag{3.2}$$

$$\underline{v}_{x-y} = \frac{2}{5}\left(v_a + \underline{a}^2 v_b + \underline{a}^4 v_c + \underline{a}^8 v_d + \underline{a}^{12} v_e\right) \tag{3.3}$$

$$\text{where}\ \underline{a} = \exp\left(j\frac{2\pi}{5}\right), \underline{a}^2 = \exp\left(j\frac{4\pi}{5}\right), \underline{a}^n = \exp\left(jn\frac{2\pi}{5}\right)$$

The space vector is a complex quantity, which represents the five-phase balanced supply with a single complex variable. Substituting equation (3.2) into equation (3.3) yields an ideal sinusoidal source, the space vector:

$$\underline{v} = V\exp(j\omega t) \tag{3.4}$$

The space vector model of a five-phase voltage source inverter can be obtained by substituting the phase voltages in equation (2.6) and determining the corresponding space vectors in the alpha-beta and x-y planes , as given in Table 3.1.

| ***Switching No.*** | ***Switching States*** | ***Space vectors in α-β plane*** | ***Space vectors in x-y plane*** |
|---|---|---|---|
| ***0*** | ***0 0 0 0 0*** | ***0*** | ***0*** |
| ***1*** | ***0 0 0 0 1*** | $\frac{2}{5}V_{DC}2\exp\left(j\frac{8\pi}{5}\right)$ | $\frac{2}{5}V_{DC}2\exp\left(j\frac{6\pi}{5}\right)$ |
| ***2*** | ***0 0 0 1 0*** | $\frac{2}{5}V_{DC}2\exp\left(j\frac{6\pi}{5}\right)$ | $\frac{2}{5}V_{DC}2\exp\left(j\frac{2\pi}{5}\right)$ |
| ***3*** | ***0 0 0 1 1*** | $\frac{2}{5}V_{DC}2\cos\left(\frac{\pi}{5}\right)\exp\left(j\frac{7\pi}{5}\right)$ | $\frac{2}{5}V_{DC}4\cos\left(\frac{2\pi}{5}\right)\exp\left(j\frac{4\pi}{5}\right)$ |
| ***4*** | ***0 0 1 0 0*** | $\frac{2}{5}V_{DC}2\exp\left(j\frac{4\pi}{5}\right)$ | $\frac{2}{5}V_{DC}2\exp\left(j\frac{8\pi}{5}\right)$ |
| ***5*** | ***0 0 1 0 1*** | $\frac{2}{5}V_{DC}4\cos\left(\frac{2\pi}{5}\right)\exp\left(j\frac{6\pi}{5}\right)$ | $\frac{2}{5}V_{DC}2\cos\left(\frac{\pi}{5}\right)\exp\left(j\frac{7\pi}{5}\right)$ |
| ***6*** | ***0 0 1 1 0*** | $\frac{2}{5}V_{DC}2\cos\left(\frac{\pi}{5}\right)\exp(j\pi)$ | $\frac{2}{5}V_{DC}4\cos\left(\frac{2\pi}{5}\right)\exp(0)$ |
| ***7*** | ***0 0 1 1 1*** | $\frac{2}{5}V_{DC}2\cos\left(\frac{\pi}{5}\right)\exp\left(j\frac{6\pi}{5}\right)$ | $\frac{2}{5}V_{DC}4\cos\left(\frac{2\pi}{5}\right)\exp\left(j\frac{7\pi}{5}\right)$ |
| ***8*** | ***0 1 0 0 0*** | $\frac{2}{5}V_{DC}2\exp\left(j\frac{2\pi}{5}\right)$ | $\frac{2}{5}V_{DC}2\exp\left(j\frac{4\pi}{5}\right)$ |
| ***9*** | ***0 1 0 0 1*** | $\frac{2}{5}V_{DC}4\cos\left(\frac{2\pi}{5}\right)\exp(0)$ | $\frac{2}{5}V_{DC}2\cos\left(\frac{\pi}{5}\right)\exp(j\pi)$ |
| ***10*** | ***0 1 0 1 0*** | $\frac{2}{5}V_{DC}4\cos\left(\frac{2\pi}{5}\right)\exp\left(j\frac{4\pi}{5}\right)$ | $\frac{2}{5}V_{DC}2\cos\left(\frac{\pi}{5}\right)\exp\left(j\frac{3\pi}{5}\right)$ |
| ***11*** | ***0 1 0 1 1*** | $\frac{2}{5}V_{DC}4\cos\left(\frac{2\pi}{5}\right)\exp\left(j\frac{7\pi}{5}\right)$ | $\frac{2}{5}V_{DC}2\cos\left(\frac{\pi}{5}\right)\exp\left(j\frac{4\pi}{5}\right)$ |
| ***12*** | ***0 1 1 0 0*** | $\frac{2}{5}V_{DC}2\cos\left(\frac{\pi}{5}\right)\exp\left(j\frac{3\pi}{5}\right)$ | $\frac{2}{5}V_{DC}4\cos\left(\frac{2\pi}{5}\right)\exp\left(j\frac{6\pi}{5}\right)$ |
| ***13*** | ***0 1 1 0 1*** | $\frac{2}{5}V_{DC}4\cos\left(\frac{2\pi}{5}\right)\exp\left(j\frac{3\pi}{5}\right)$ | $\frac{2}{5}V_{DC}2\cos\left(\frac{\pi}{5}\right)\exp\left(j\frac{6\pi}{5}\right)$ |

| | | | |
|---|---|---|---|
| ***14*** | ***0 1 1 1 0*** | $\frac{2}{5}V_{DC}\,2\cos\left(\frac{\pi}{5}\right)\exp\left(j\frac{4\pi}{5}\right)$ | $\frac{2}{5}V_{DC}\,4\cos\left(\frac{2\pi}{5}\right)\exp\left(j\frac{3\pi}{5}\right)$ |
| ***15*** | ***0 1 1 1 1*** | $\frac{2}{5}V_{DC}\,2\exp(j\pi)$ | $\frac{2}{5}V_{DC}\,2\exp(j\pi)$ |
| ***16*** | ***1 0 0 0 0*** | $\frac{2}{5}V_{DC}\,2\exp(j0)$ | $\frac{2}{5}V_{DC}\,2\exp(j\pi)$ |
| ***17*** | ***1 0 0 0 1*** | $\frac{2}{5}V_{DC}\,2\cos\left(\frac{\pi}{5}\right)\exp\left(j\frac{9\pi}{5}\right)$ | $\frac{2}{5}V_{DC}\,4\cos\left(\frac{2\pi}{5}\right)\exp\left(j\frac{8\pi}{5}\right)$ |
| ***18*** | ***1 0 0 1 0*** | $\frac{2}{5}V_{DC}\,4\cos\left(\frac{2\pi}{5}\right)\exp\left(j\frac{8\pi}{5}\right)$ | $\frac{2}{5}V_{DC}\,2\cos\left(\frac{\pi}{5}\right)\exp\left(j\frac{\pi}{5}\right)$ |
| ***19*** | ***1 0 0 1 1*** | $\frac{2}{5}V_{DC}\,2\cos\left(\frac{\pi}{5}\right)\exp\left(j\frac{7\pi}{5}\right)$ | $\frac{2}{5}V_{DC}\,4\cos\left(\frac{2\pi}{5}\right)\exp\left(j\frac{\pi}{5}\right)$ |
| ***20*** | ***1 0 1 0 0*** | $\frac{2}{5}V_{DC}\,4\cos\left(\frac{2\pi}{5}\right)\exp\left(j\frac{2\pi}{5}\right)$ | $\frac{2}{5}V_{DC}\,2\cos\left(\frac{\pi}{5}\right)\exp\left(j\frac{9\pi}{5}\right)$ |
| ***21*** | ***1 0 1 0 1*** | $\frac{2}{5}V_{DC}\,4\cos\left(\frac{2\pi}{5}\right)\exp\left(j\frac{9\pi}{5}\right)$ | $\frac{2}{5}V_{DC}\,2\cos\left(\frac{\pi}{5}\right)\exp\left(j\frac{7\pi}{5}\right)$ |
| ***22*** | ***1 0 1 1 0*** | $\frac{2}{5}V_{DC}\,4\cos\left(\frac{2\pi}{5}\right)\exp(j\pi)$ | $\frac{2}{5}V_{DC}\,2\cos\left(\frac{\pi}{5}\right)\exp(j0)$ |
| ***23*** | ***1 0 1 1 1*** | $\frac{2}{5}V_{DC}\,2\exp\left(j\frac{7\pi}{5}\right)$ | $\frac{2}{5}V_{DC}\,2\exp\left(j\frac{9\pi}{5}\right)$ |
| ***24*** | ***1 1 0 0 0*** | $\frac{2}{5}V_{DC}\,2\cos\left(\frac{\pi}{5}\right)\exp\left(j\frac{\pi}{5}\right)$ | $\frac{2}{5}V_{DC}\,4\cos\left(\frac{2\pi}{5}\right)\exp\left(j\frac{2\pi}{5}\right)$ |
| ***25*** | ***1 1 0 0 1*** | $\frac{2}{5}V_{DC}\,2\cos\left(\frac{\pi}{5}\right)\exp(j0)$ | $\frac{2}{5}V_{DC}\,4\cos\left(\frac{2\pi}{5}\right)\exp(j\pi)$ |
| ***26*** | ***1 1 0 1 0*** | $\frac{2}{5}V_{DC}\,4\cos\left(\frac{2\pi}{5}\right)\exp\left(j\frac{\pi}{5}\right)$ | $\frac{2}{5}V_{DC}\,2\cos\left(\frac{\pi}{5}\right)\exp\left(j\frac{2\pi}{5}\right)$ |
| ***27*** | ***1 1 0 1 1*** | $\frac{2}{5}V_{DC}\,2\exp\left(j\frac{9\pi}{5}\right)$ | $\frac{2}{5}V_{DC}\,2\exp\left(j\frac{3\pi}{5}\right)$ |
| ***28*** | ***1 1 1 0 0*** | $\frac{2}{5}V_{DC}\,2\cos\left(\frac{\pi}{5}\right)\exp\left(j\frac{2\pi}{5}\right)$ | $\frac{2}{5}V_{DC}\,4\cos\left(\frac{2\pi}{5}\right)\exp\left(j\frac{9\pi}{5}\right)$ |

| | | | |
|---|---|---|---|
| ***29*** | ***1 1 1 0 1*** | $\frac{2}{5}V_{DC}2\exp\left(j\frac{\pi}{5}\right)$ | $\frac{2}{5}V_{DC}2\exp\left(j\frac{7\pi}{5}\right)$ |
| ***30*** | ***1 1 1 1 0*** | $\frac{2}{5}V_{DC}2\exp\left(j\frac{3\pi}{5}\right)$ | $\frac{2}{5}V_{DC}2\exp\left(j\frac{\pi}{5}\right)$ |
| ***31*** | ***1 1 1 1 1*** | ***0*** | ***0*** |

*Table 3. 1 Space vector table of phase voltages for a five-phase VSI*

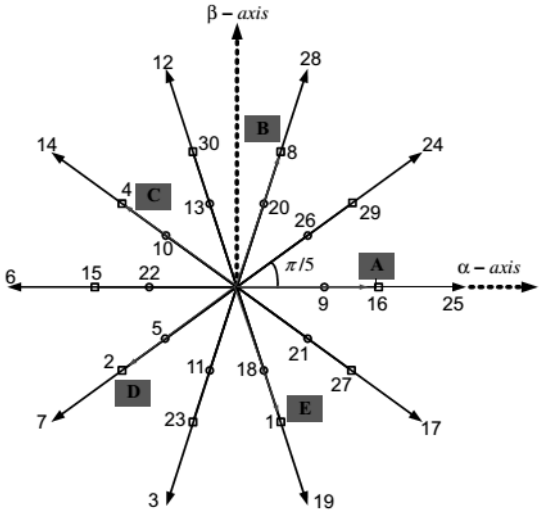


*Figure 3. 3: Phase voltage space vector α-β plane*

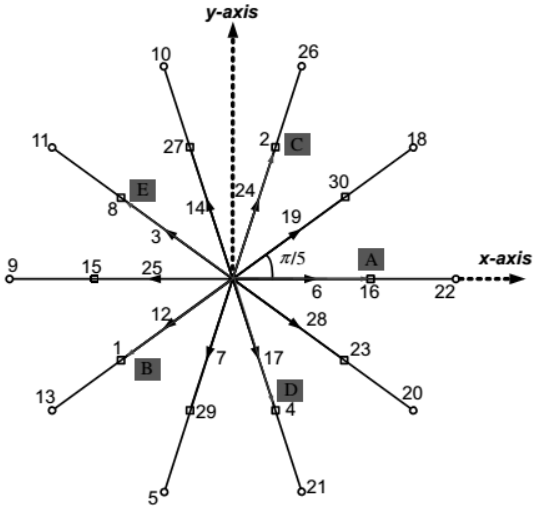


*Figure 3. 4: Phase voltage space vector x-y plane*

### 3.3.1 Application of the large space vectors only

The SVPWM scheme discussed in this section considers the outer-most decagon of space vectors in α- β plane. The input reference voltage vector is synthesized from two active neighboring and zero space vectors. To calculate the time of application of different vectors, consider Fig. 3.5, depicting the position of different available space vectors and the reference vector in the first sector.

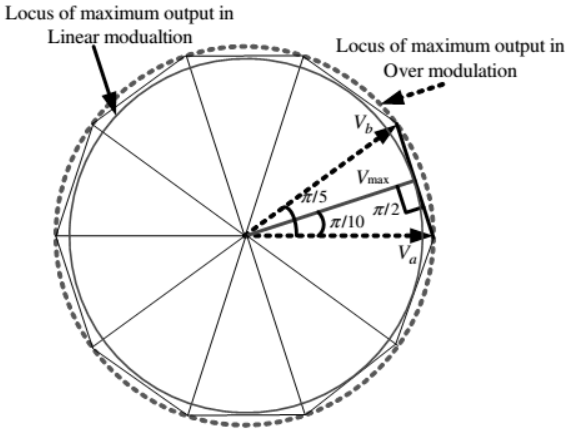


*Figure 3. 5: Maximum possible output in SVPWM for a five-phase VSI*

When the reference voltage is in sector I, the reference voltage can be synthesized by using the vectors $v_a$,$v_b$, and $v_o$(zero vector), applied for time $t_a$,$t_b$, and $t_o$, respectively. Hence, using the equal volt-second principle, for sector I. The time of application of active space voltage vectors is found from Fig. 3.5 as

$$\underline{v_s}^{*} t_s = \underline{v_a}\, t_a + \underline{v_b}\, t_b \tag{3.5}$$

In Cartesian form, this equation can be written as:

$$\left|\underline{v_s^*}\right|(\cos(\alpha)+ j\sin(\alpha))t_s = \left|\underline{v_a}\right|(\cos(0)+ j\sin(0))t_a + \left|\underline{v_b}\right|\left(\cos\left(\frac{\pi}{5}\right)+ j\sin\left(\frac{\pi}{5}\right)\right)t_b \tag{3.6}$$

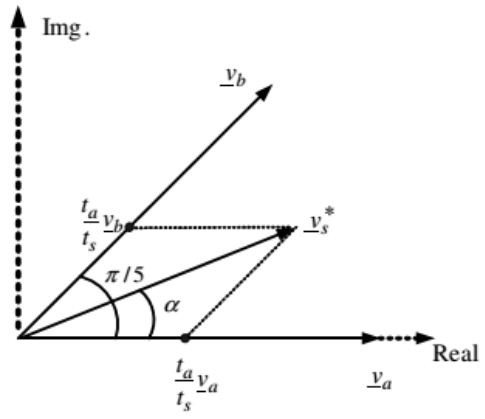


*Figure 3. 6: Principle of space vector time calculation for a five-phase VSI.*

Now equating the real and imaginary parts, the following relations are obtained:

$$t_a = \frac{|v_s^*|}{V_l \sin(\pi/5)} t_s \sin\left(\frac{\pi}{5}k - \alpha\right) \tag{3.7}$$

$$t_b = \frac{|v_s^*|}{V_l \sin(\pi/5)} t_s \sin\left(\alpha - (k-1)\frac{\pi}{5}\right) \tag{3.8}$$

$$t_o = t_s - t_a - t_b \tag{3.9}$$

Where k is the number of the sector, symbol $\underline{v}_s^*$ denotes the reference voltage space vector, Indices "l" stand for large vector. The largest possible fundamental peak voltage magnitude that may be achieved using this scheme corresponds to the radius of the largest circle that can be inscribed within the decagon. The circle is tangential to the mid-point of the lines connecting the ends of the active space vectors. Thus the maximum fundamental phase to neutral peak output voltage is:

$$V_{max} = (2/5)2\cos\left(\frac{\pi}{5}\right)\cos\left(\frac{\pi}{10}\right) V_{DC} = 0.61554\, V_{DC} \tag{3.10}$$

The maximum peak fundamental output in ten step mode is, from expression (2.71), given with $V_{max,ten\ step} = \frac{2}{\pi} V_{DC}$ . Thus the ratio of the maximum possible fundamental output voltage with SVPWM and in ten-step mode is $V_{max}/V_{max,ten\ step} = .\ 0.96689$

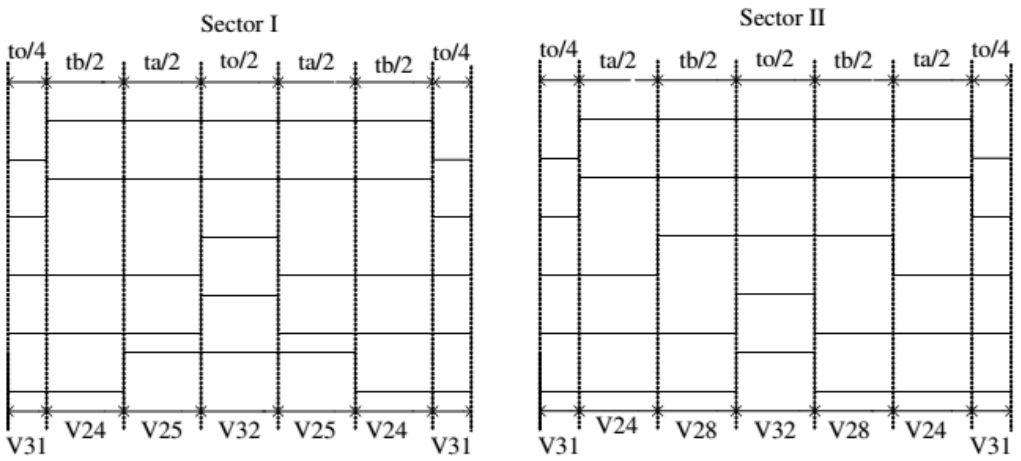


*Figure 3. 7: Switching pattern for SVPWM using only two active vectors*

### 3.3.2 Combined application of medium and large space vectors

Use of four active space vectors per switching period requires the calculation of four application times, labeled here as $t_{al}$, $t_{bl}$, $t_{am}$, $t_{bm}$. The expressions used for calculation of dwell times of various space vectors are:

$$\underline{v}_s^* t_s = \underline{v}_{al}\, t_{al} + \underline{v}_{bl}\, t_{bl} + \underline{v}_{am}\, t_{am} + \underline{v}_{bm}\, t_{bm} \tag{3.11}$$

Where

$$\underline{v}_{al} = \underline{v}_{bl} = \underline{v}_l = \frac{2}{5} V_{DC} 2\cos(\pi/5) \tag{3.12}$$

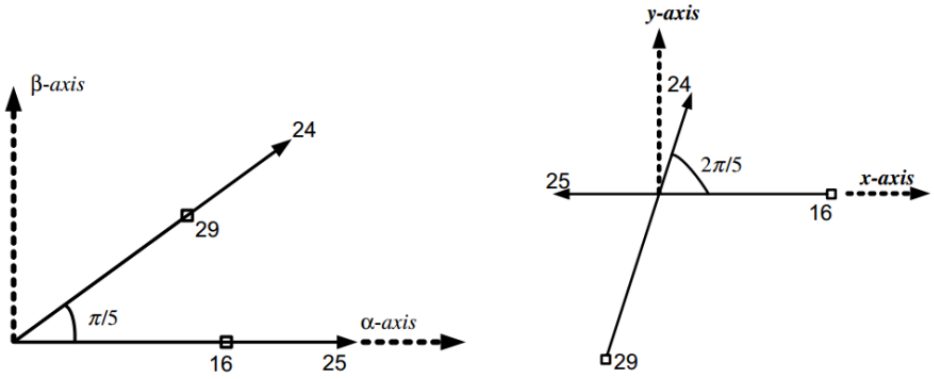


*Figure 3. 8: Principle of space vector time calculation for a five-phase VSI.*

$$\underline{v}_{am} = \underline{v}_{bm} = \underline{v}_m = \frac{2}{5} V_{DC} \tag{3.13}$$

and

$$\frac{t_{al}}{t_{am}} = \frac{t_{bl}}{t_{bm}} = \frac{v_l}{v_m} = \tau = 1.618 \tag{3.14}$$

Separating the real and imaginary parts of equation and substituting equation, the following equations result:

$$t_{al} = \frac{|v_s^*|}{V_m \sin(\pi/5)} \left( \frac{\tau}{1+\tau^2} \right) t_s sin\left( \frac{\pi}{5} k - \alpha \right) \tag{3.15}$$

$$t_{bl} = \frac{|v_s^*|}{V_m \sin(\pi/5)} \left( \frac{\tau}{1+\tau^2} \right) t_s sin\left( \alpha - (k-1)\frac{\pi}{5} \right) \tag{3.16}$$

$$t_{am} = \frac{|v_s^*|}{V_m \sin(\pi/5)} \left( \frac{\tau}{1+\tau^2} \right) t_s sin\left( \frac{\pi}{5} k - \alpha \right) \tag{3.17}$$

$$t_{bm} = \frac{|v_s^*|}{V_m \sin(\pi/5)} \left( \frac{\tau}{1+\tau^2} \right) t_s sin\left( \alpha - (k-1)\frac{\pi}{5} \right) \tag{3.18}$$

$$t_o = t_s - t_{al} - t_{bl} - t_{am} - t_{bm} \tag{3.19}$$

Where $t_a = t_{al} + t_{am}$ ,$t_b = t_{bl} + t_{bm}$. This allocates 61.8% more dwell time to a large space vector compared to a medium space vector, thus satisfying the constraints of producing zero average voltage in the x-y plane. The constraint imposed on the time of application of each vector is that they cannot be less than zero, and also the sum of time of application of active and zero vectors cannot exceed the switching time. With these constraints, the maximum possible output with this approach is $0.5257V_{DC}$, which is almost 16% less than with the previous method.

After locating the reference location and calculating the dwell time, the next step in SVPWM implementation is the determination of the switching sequence. The requirement is the minimum number of switching's to reduce switching loss, ideally one power switch should turn 'ON' and turn 'OFF' in one switching period.

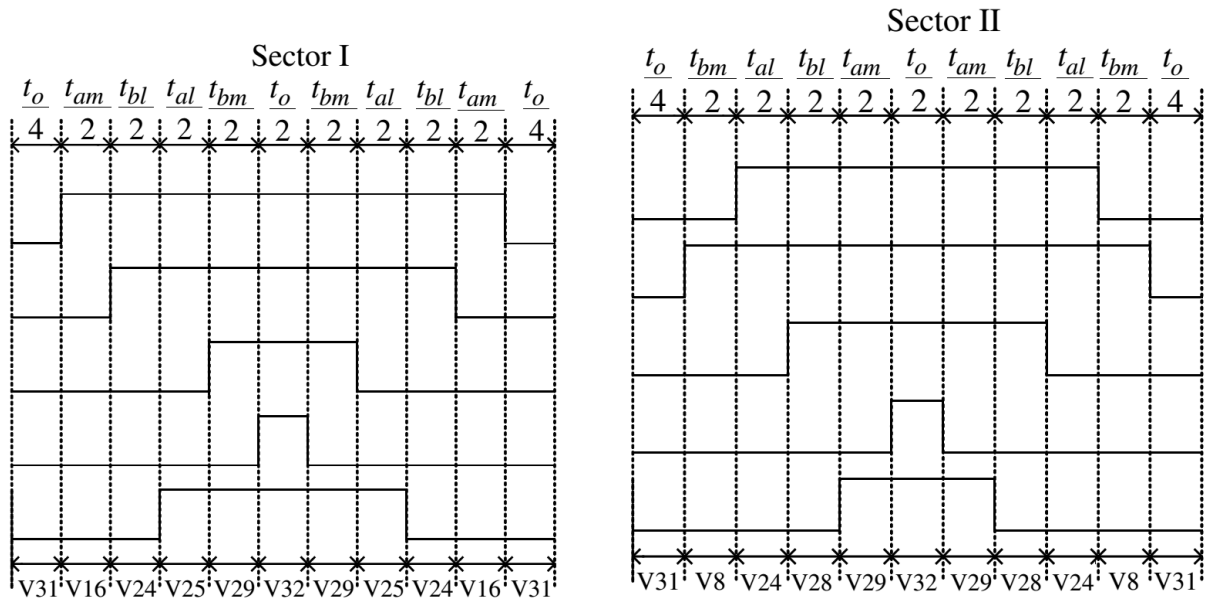


*Figure 3. 9: Switching pattern for SVPWM using four active vectors*

## 3.4 PI Control Scheme

PI controller will eliminate forced oscillations and steady state error resulting in operation of on-off controller and P controller respectively. However, introducing integral mode has a negative effect on speed of the response and overall stability of the system. Thus, PI controller will not increase the speed of response.

The dynamics of induction motor (IM) is traditionally represented by differential equations. The space-vector concept [13] is used in the mathematical representation of IM state variables such as voltage, current, and flux. By using stator field orientation, the torque and stator flux must become parts of a complex number, where the magnitude of the stator flux is the real component and the torque is the imaginary component. Hence, the reference signals and the error become a complex number. Thus, the PI regulators presented in the section [23] has the function to generate a voltage reference space vector using the stator flux-torque error vector.

In order to tune the PI regulator it is necessary the closed-loop complex transfer function of the controlled induction motor. The complex transfer function of the controlled induction motor was also used to tune a complex gain controller in which has been presented in [7].

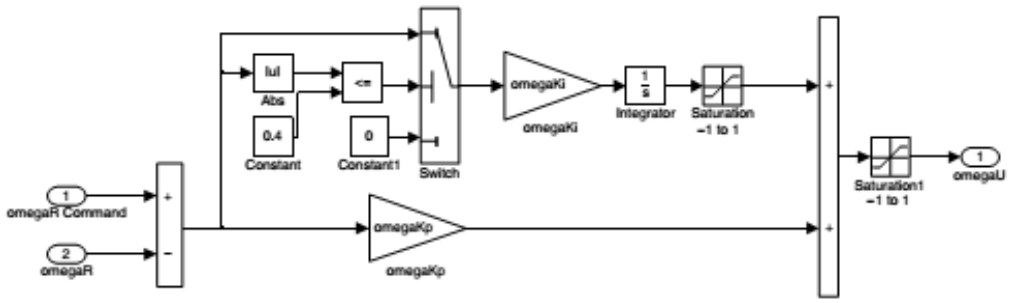


*Figure 3. 10: Limited authority PI control systems model*

# CHAPTER FOUR

## CONTROLLER DESIGN

### 4.1 Introduction

The basis of scalar control is the selection of the speed of the common reference frame. In v/f control scheme the speed of the reference frame is selected as equal to the rated speed of the induction motor. Due to the lack of data for multi-phase machines, it is assumed that per-phase parameters and ratings of the multi-phase induction machines are the same as for the three-phase machine.

### 4.2 Parameter Selection of the motor

The basis for all the simulations is a two-pole, 50 Hz three-phase induction machine, with magnetizing inductance of 0.42 H and rated torque of 1.066 Nm. Rated rotor flux (RMS) for this benchmark three-phase machine is equal to 0.5683 Wb [Jones (2005)]. Due to the use of power invariant transformation the following values of rotor flux and rated torque are used for simulation:

Five-phase machine:

$$\psi_r^* = \sqrt{5}\psi_{rn} = 1.2707\ wb$$

$$T_{en} = 5T_n = 8.33 Nm$$

The simulation model is developed in a Matlab/Simulink environment. The simulation parameters for five-phase induction motor are shown in Table 4.1.

| No | Description | Parameter | Value | Unit |
|---|---|---|---|---|
| 1 | Stator resistance | $R_s$ | 0.045 | Ω |
| 2 | Rotor resistance | $R_r$ | 0.045 | Ω |
| 3 | Stator inductance | $L_s$ | 1.927 | H |
| 4 | Rotor inductance | $L_r$ | 1.927 | H |
| 5 | Mutual inductance | $L_m$ | 1.85 | H |
| 6 | Inertia | J | 59 | $Kg.m^2$ |
| 7 | Rated speed | ω | 1500 | rpm |
| 8 | No of poles | P | 4 | - |

*Table 4. 1: electrical and mechanical parameter of the motor*

### 4.3 Design of PI controller

PI speed controller is considered next. There are two types of PI speed controllers, a continuous one and a discrete one. The type of the speed controller used in this specific simulation is continuous type speed controller. The design of continuous speed controller is presented here. For this purpose, and having in mind that the inverter current control will be performed in the stationary reference frame using hysteresis or ramp comparison technique, the whole current control loop is approximated with unity gain and zero time delay. The structure of the speed control loop is then as shown in Fig. (4.1).

$$T_e - T_L = \frac{J}{P}\frac{d\omega}{dt} \tag{4.1}$$

$$\omega = \frac{P}{J}\int T_e dt \tag{4.2}$$

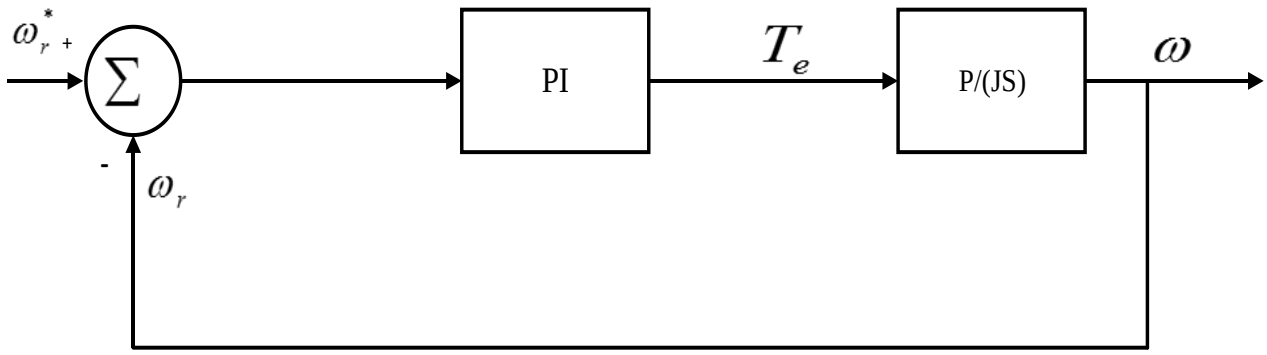


*Figure 4. 1: PI speed controller*

The transfer function of the PI speed controller is:

$$G_{PI}(S) = K_P\left(1 + \frac{1}{S\tau_i}\right) = K_P + K_I\frac{1}{S} \tag{4.3}$$

The characteristic equation of the above speed control loop is solved for

$$1 + G_{PI}(S)H(S) = 0 \tag{4.4}$$

Where according to Fig. (4.1)

$$H(S) = \frac{1}{SJ/P} \tag{4.5}$$

The parameters are P=2, J=0.03 kgm$^2$. Hence the characteristic equation is:

$$S^2 + 66.67K_P S + 66.67K_I = 0 \tag{4.6}$$

The coefficients in the above equation are equated with those in the following equation, which defines the desired closed loop dynamics in terms of the damping ratio $\xi$ and natural frequency $\omega_0$:

$$S^2 + 2\xi\omega_0 S + \omega_0^{\ 2} = 0 \tag{4.7}$$

Damping ratio is selected as 0.707. The natural frequency for the speed control loop is dependent on the bandwidth of the inner current control loop. Maximum practical value of the current control loop bandwidth in the case of ramp frequency is 1 kHz. For the purpose of the speed controller design, current loop bandwidth is taken as one tenth of the maximum value (i.e. as 100 Hz). Taking the speed control bandwidth as one tenth of this value (10 Hz) and approximating the natural frequency with the bandwidth, one has

$$\omega_0 = 2\pi * 10 = 62.8318 \text{ rad/s} \tag{4.8}$$

Substitution of the damping ratio and natural frequency values into (4.4) and comparison with (4.5) yields the following values for the speed controller parameters:

| $K_P$ | $K_I$ | $\tau_i$ (S) |
|---|---|---|
| 1.332 | 59.214 | 0.0225 |

*Table 4. 2: PI coefficients*

The step response of the PI controller

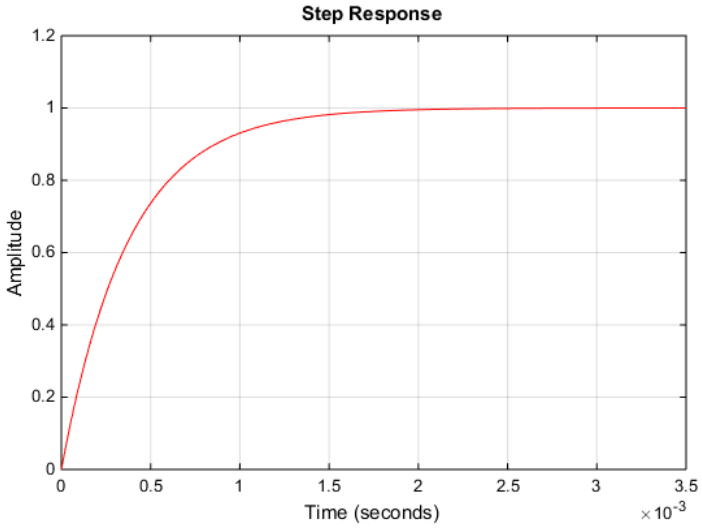


The following result is obtained from the simulation of the PI controller:

| Rise Time(s) | Settling Time(s) | Over shoot (%) | Peak |
|---|---|---|---|
| 8.2365e-04 | 0.0015 | 0.0067 | 1.0001 |

*Table 4.3 result of the step response*

## 4.4 Design of scalar controller

In this type of control, a constant ratio between the voltage magnitude and frequency is maintained. This is to keep it constant and is the optimal flux in the machine.

$$U_{sd} = R_S i_{sd} + \frac{d\psi_{sd}}{d\tau} - \omega_a \psi_{sq} \tag{4.9}$$

$$U_{sq} = R_S i_{sq} + \frac{d\psi_{sq}}{d\tau} - \omega_a \psi_{sd} \tag{4.10}$$

It is assumed that the co-ordinate system is connected with stator current, hence:

$$\psi_{sd} = |\psi_s| \tag{4.11}$$

$$\psi_{sd} = 0 \tag{4.12}$$

Which is a steady state would be

$$\frac{d\psi_{sd}}{d\tau} = 0 \tag{4.13}$$

Therefore:

$$U_{sd} = R_S i_{sd} \tag{4.14}$$

$$U_{sq} = R_S i_{sq} + \omega_a \psi_{sd} \tag{4.15}$$

The voltage vector magnitude is

$$|U_s| = \sqrt{U^2_{sd} + U^2_{sq}} \tag{4.16}$$

$$|U_s| = \sqrt{(R_s i_{sd})^2 + (R_s i_{sq}) + (\omega_a \psi_{sd})^2 + 2.R_s i_{sq}.\omega_a \psi_{sd}} \tag{4.17}$$

Neglecting stator resistance, the following is achieved:

$$|U_s| = \sqrt{(\omega_a \psi_{sd})^2} \tag{4.18}$$

Keeping constant motor flux magnitude at rated value (in per unit, this is 1), the following is correct:

$$|\psi_s| = 1 \tag{4.19}$$

Therefore:

$$|U_s| = \sqrt{(\omega_a)^2} \tag{4.20}$$

Where

$$\omega_a = 2\pi f \tag{4.21}$$

The control law of five phase drive

$$V = K\left(\frac{V_n}{f_n}\right) f + V_0 \tag{4.22}$$

Thus, in V/f control, a constant ratio between the voltage magnitude and frequency is maintained. This is to keep constant and optimal flux in the machine. Therefore, the stator voltage is adjusted in accordance to the following rule:

$$\begin{cases} (V_r - V_0)\dfrac{f}{f_r} + V_0 & \text{for } f < f_r \\ V_r & \text{for } f \geq f_r \end{cases} \tag{4.23}$$

Where $V_s$ is the stator voltage, $V_r$ is rated stator voltage, $V_0$ denotes the rms value of the stator voltage at zero frequency, $f_r$ is rated frequency.

# CHAPTER FIVE

## SIMULATION RESULTS AND DISCUSSION

### 5.1 Steady state performance of the five-phase induction motor drive

This section illustrates the steady state performance of the five-phase induction motor drive. At first the results for the five-phase induction motor are presented. This is followed by the presentation of the performance for constant v/f speed controller.

Input five-phase Voltage to the stator of machine

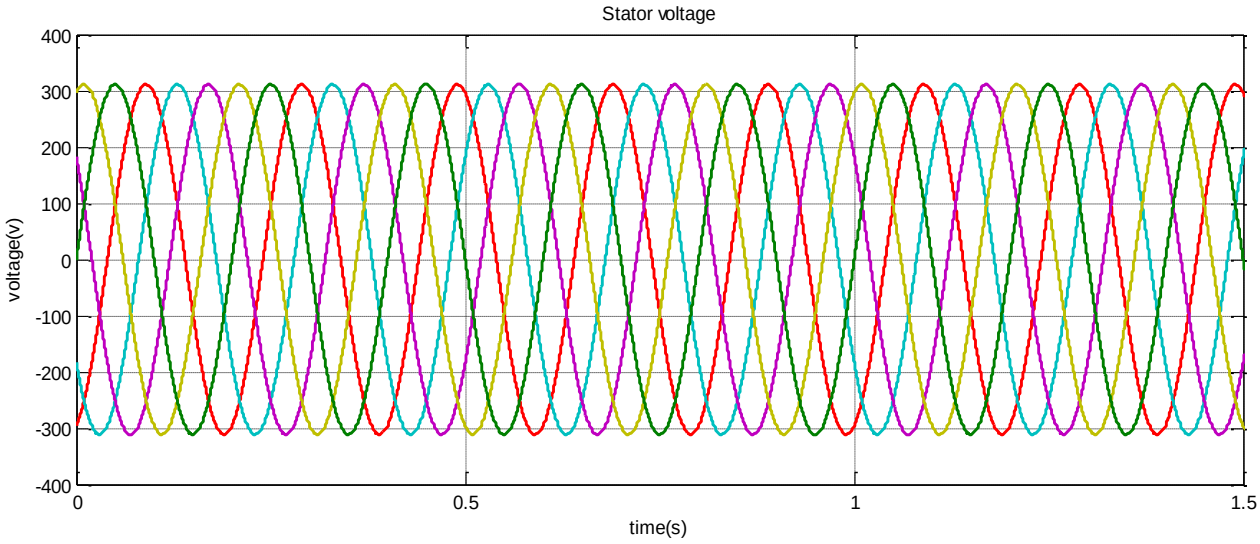


*Figure 5. 1 stator voltages*

To observe the behavior of the machine under loaded conditions, a rated load of 8.33 Nm is applied to the motor shaft at a time instant of 1 sec. The load is applied once the motor reaches a steady-state condition after excitation and acceleration transients. The resulting waveforms are shown in the following Figures.

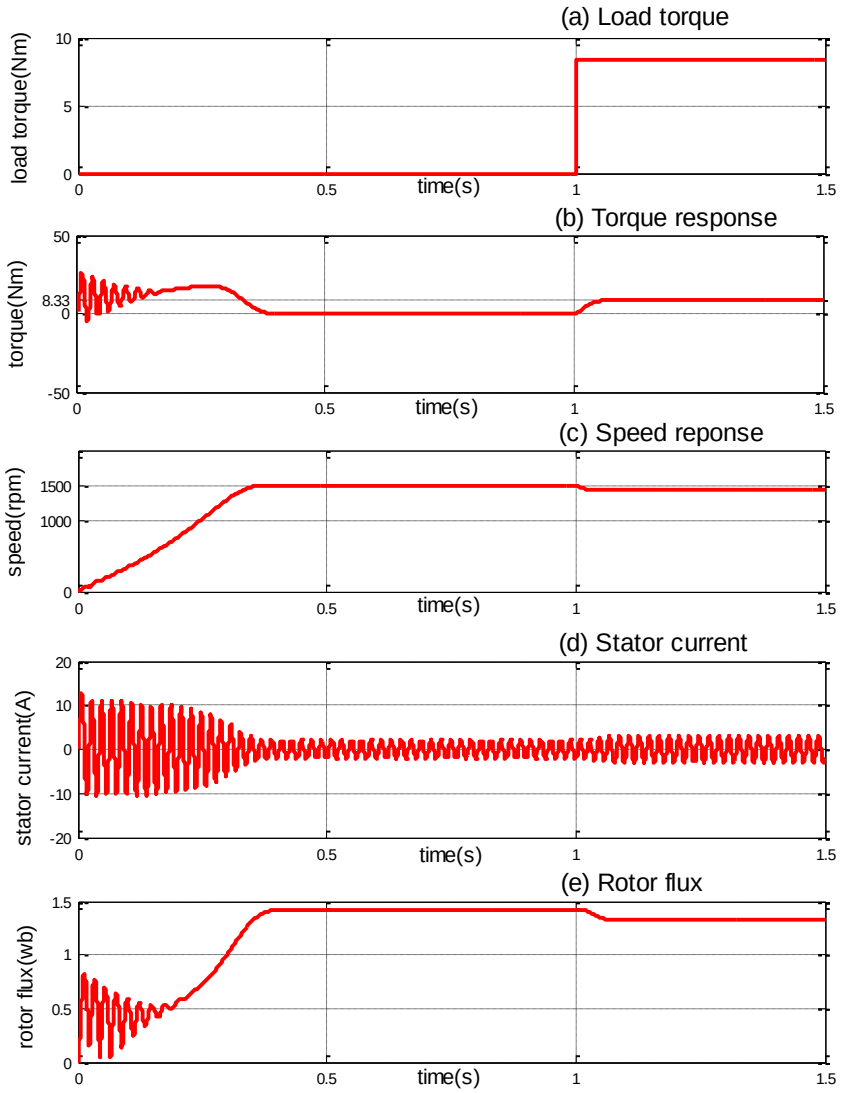


*Figure 5. 2: responses of the machine under no load and rated load condition*

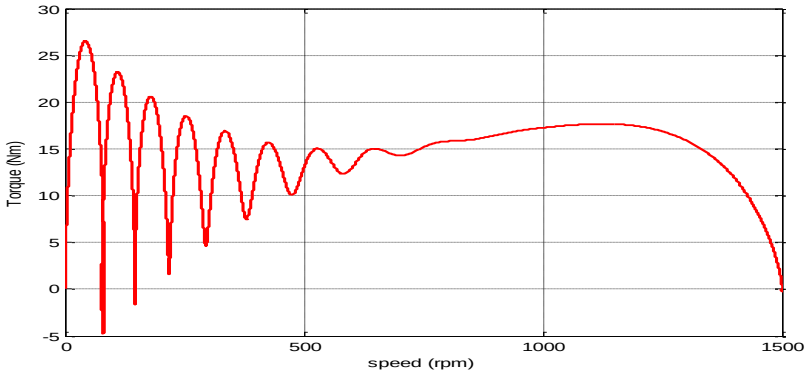


*Figure 5. 3:Torque versus speed response of five-phase motor under no-load*

Speed reversal of the motor study is also simulated and the resulting responses is shown in Fig. (5.4.)

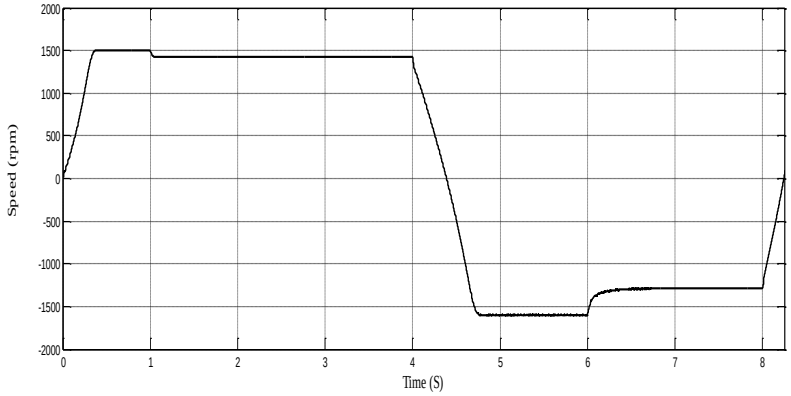


*Figure 5. 4: Speed reversal of the motor*

## 5.2 SVPWM Result

The SVPWM can be developed in MATLAB/Simulink by using different approaches. The model presented here uses the Simulink and MATLAB function block. The MATLAB/Simulink model is presented in Figure B.1. The five-phase voltage reference is generated using the 'sine wave' generator and then transformed into alpha-beta and x-y components.

The reference space vector magnitude and angle is thus generated from the 'reference voltage generator' block. The magnitude is constant, while the angle changes from 0 to pi and then pi to 0 as a saw tooth waveform. The angle is held for one sample time, so as to keep its value constant during the calculation of times of application of vectors. Another repetitive signal (time [0 Ts], amplitude [0 Ts]) is used to compare with the angle to determine the location of the reference signal.

The MATLAB function block contains the switching table and sector determination algorithm. The MATLAB function block outputs the switching functions and is given to the five-phase inverter model. The algorithm inside the MATLAB function block can be changed to implement two-vector or four-vector SVPWM.

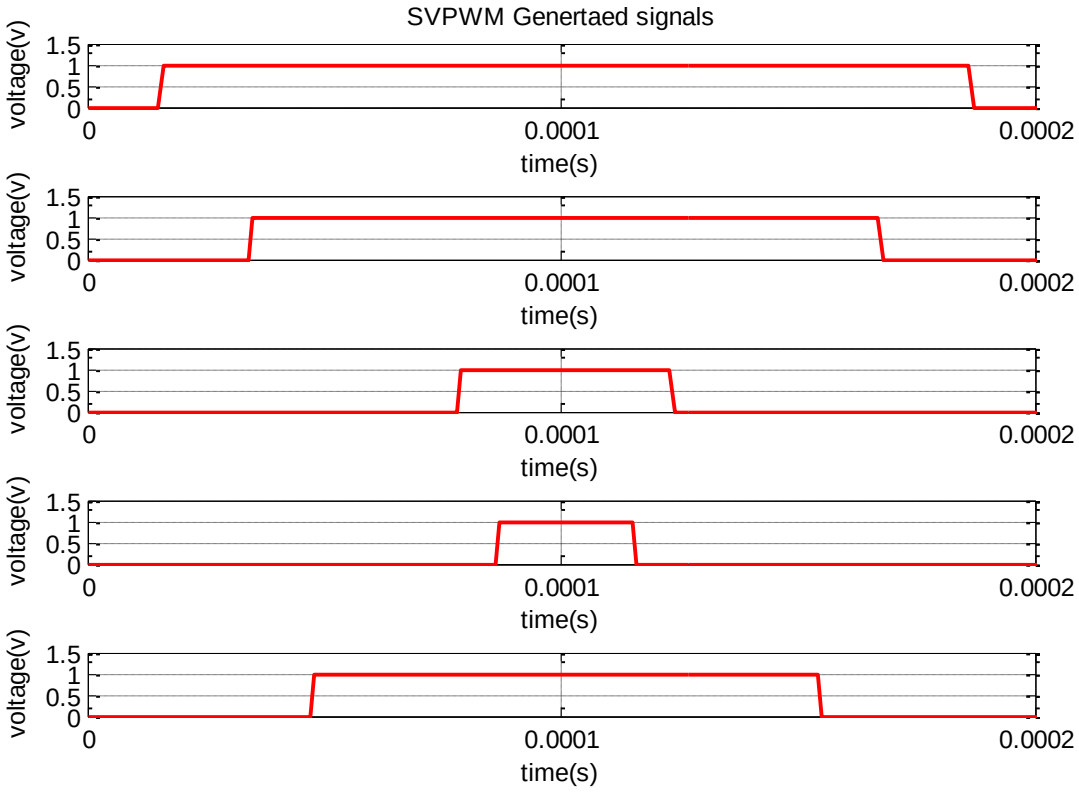


*Figure 5. 5: switching pattern for sector I for the application of four active vectors*

Simulation results are shown for two SVPWM techniques, using two active vectors (Figure 3.14) and using four active vectors (Figure 3.15). The fundamental frequency is kept at 50 Hz, the switching frequency is chosen as 5 kHz, the output is set at maximum value (0.6115 $V_{dc}$ for two vectors case and 0.5257 $V_{dc}$ for four vectors case), and the DC link voltage $V_{dc}$ is set to 1 p.u. The output phase voltages are distorted if only two active vectors are employed for SVPWM. The distortion appears due to the presence of the x-y plane vectors, as evident from Figure 3.12. The phase voltages are completely sinusoidal when using four active vectors for the implementation of SVPWM. This is due to the fact that the x-y components are completely eliminated. The value of THD drops while shifting from a two active vector application (85%) to a four active vector application (70%) in one switching period.

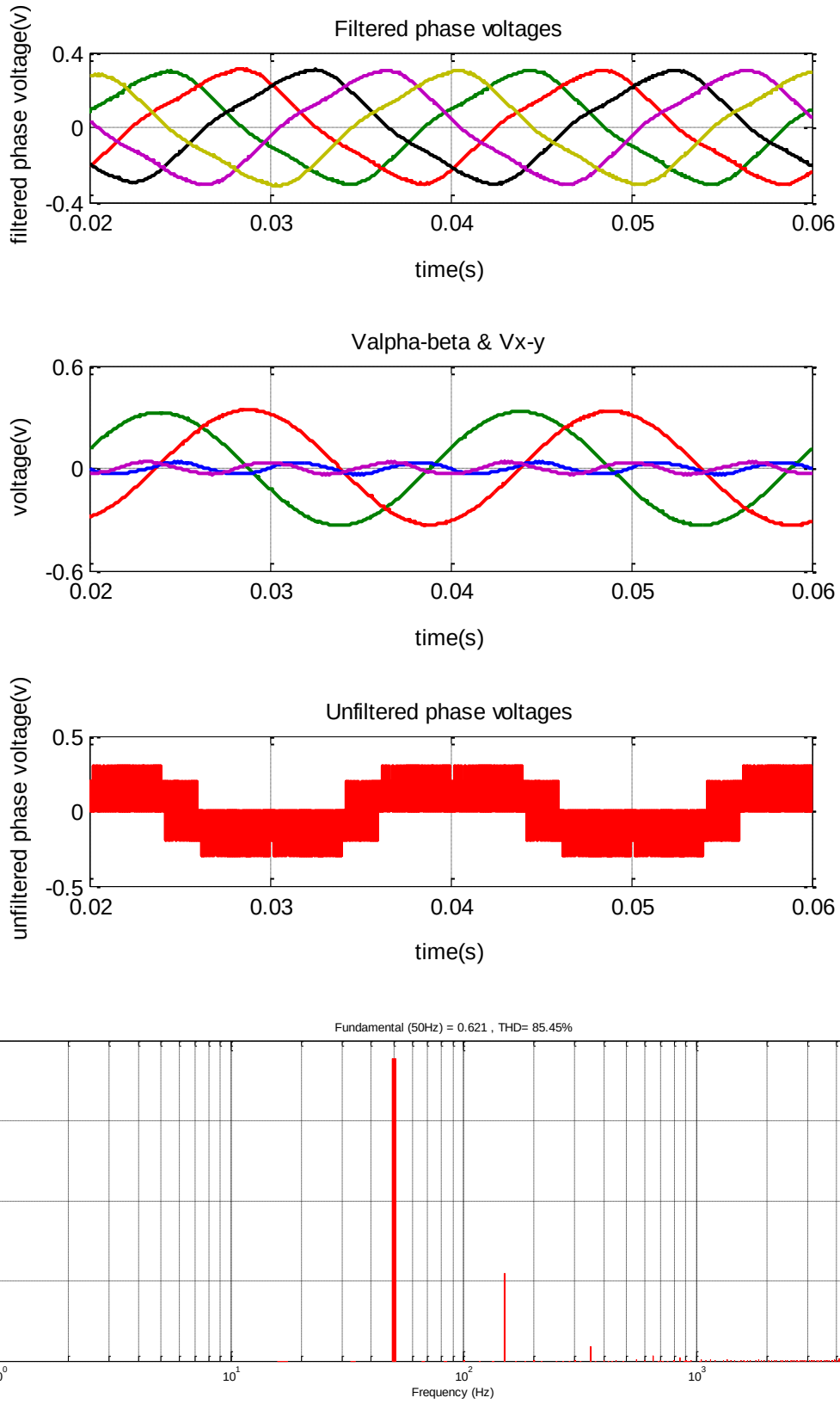


*Figure 5. 6: application of two active space vectors*

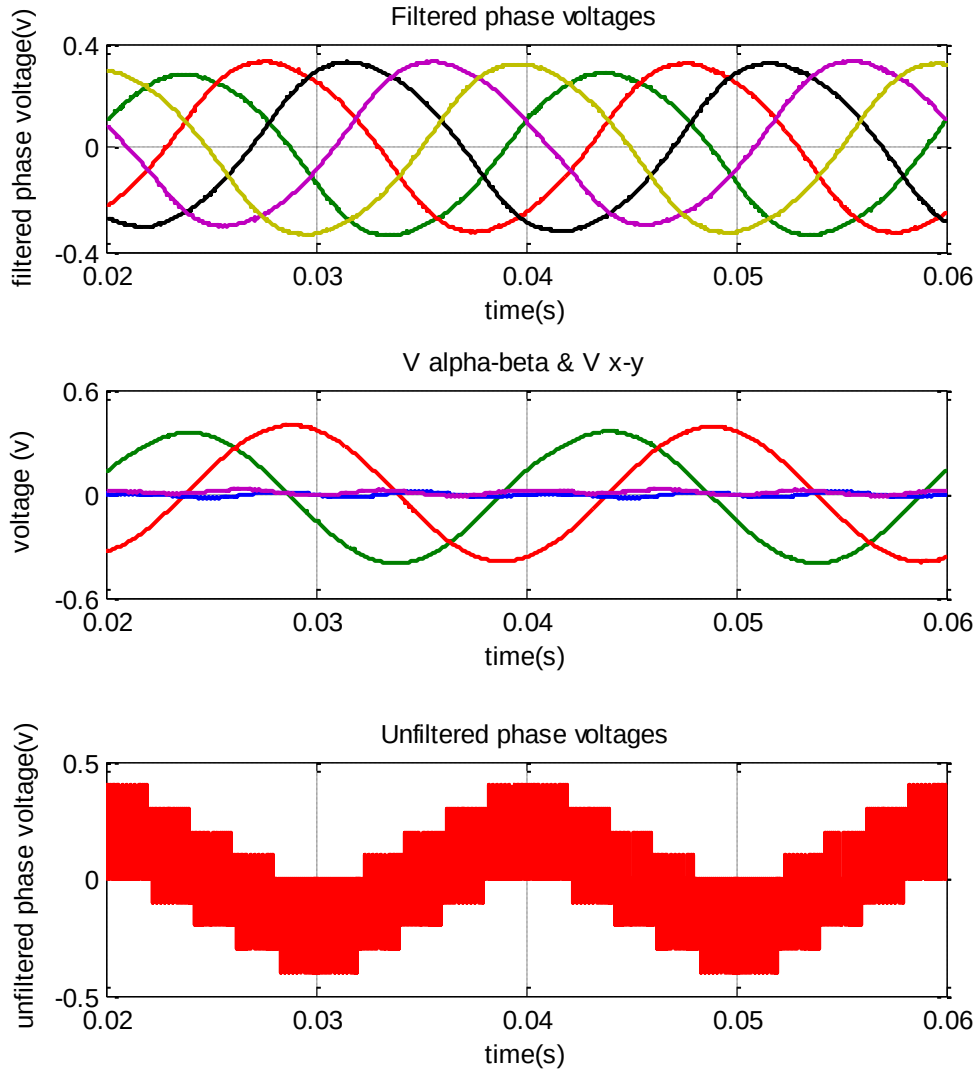


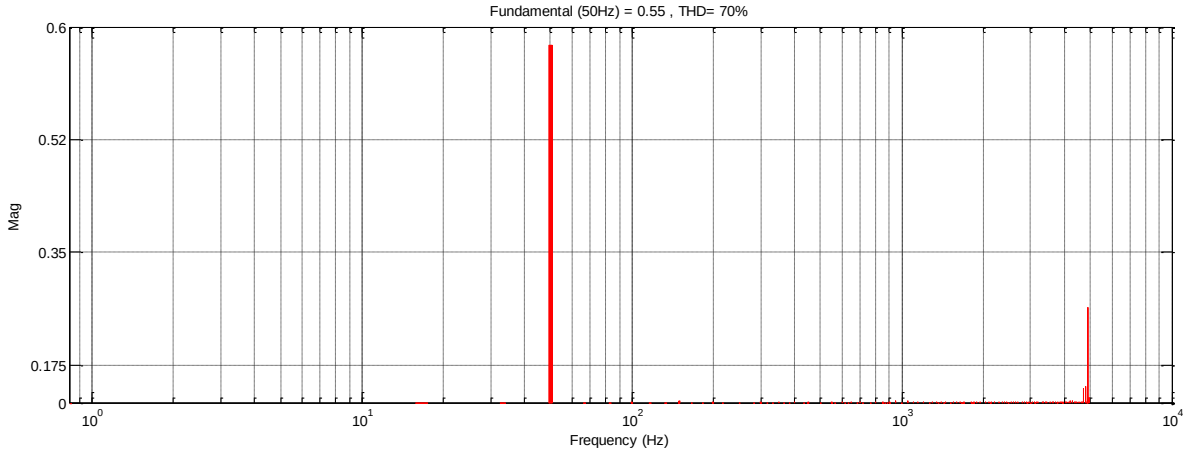


*Figure 5. 7: application of four active space vectors*

## 5.3 Fault tolerance results

Fault tolerant feature of the 5-phase induction motor is observed from 1st and 1st and 5th stator windings opened condition is shown in Figs. 5.8 and 5.9. It is seen that the number of lost phase increases, the starting current of the rest of the phases increases and rated torque decreases gradually.

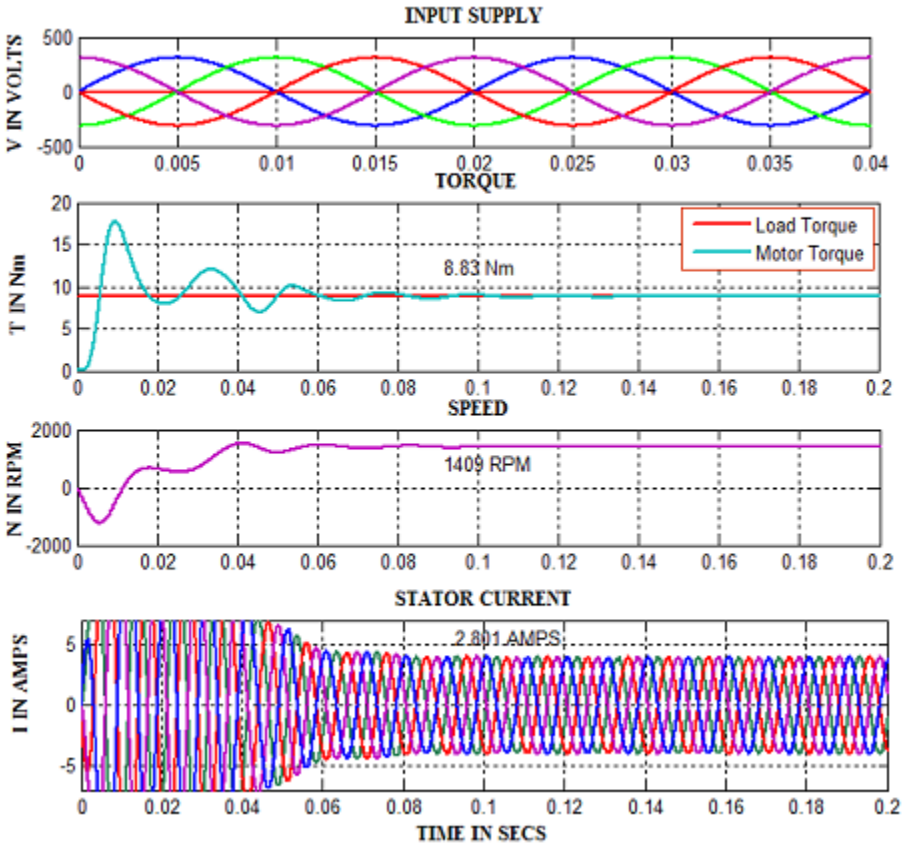


*Figure 5. 8: Fault tolerant results of 5-phase induction motor with one (1st) of the phase is opened*

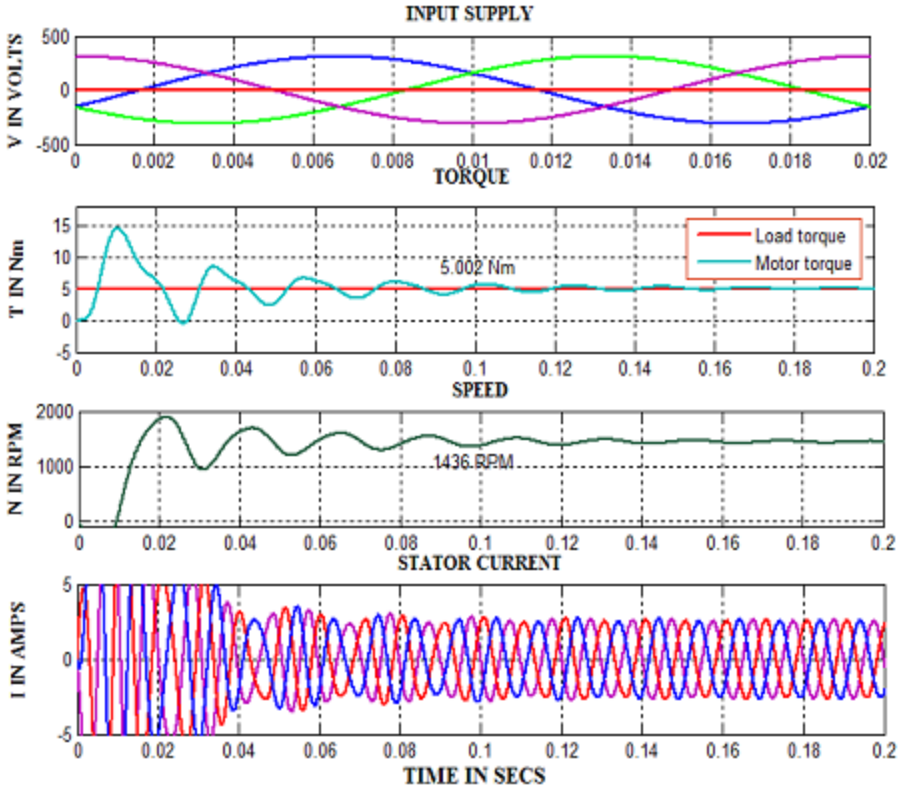


*Figure 5. 9: Fault tolerant simulation results of 5-phaseinduction motor with two (1st and 5 th) of the phases are opened*

## 5.4 Torque pulsation

It is realized that the five-phase induction motor drive systems offered some distinct advantages over three-phase drive system counterparts. Torque pulsation will be reduced except those pulsations which are due to slot permeance effects. The simulation is incorporated with the same specification of three phase and five phase induction motors. The simulation result is illustrated as in fig.(5.22)and fig.(5.23) . Torque pulsation stays for 0.2 sec in five phase induction motor and stays more than 0.5 sec for its three phase counterpart.

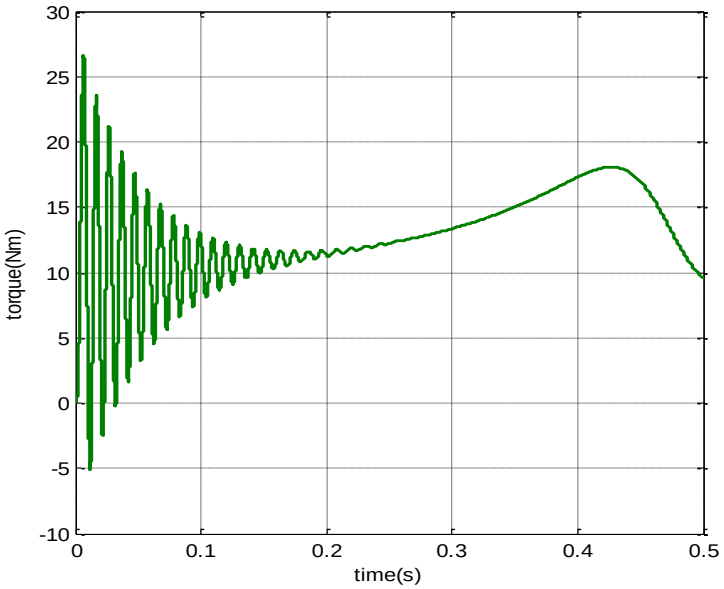


*Figure 5. 10:Torque pulastion for five phase induction motor*

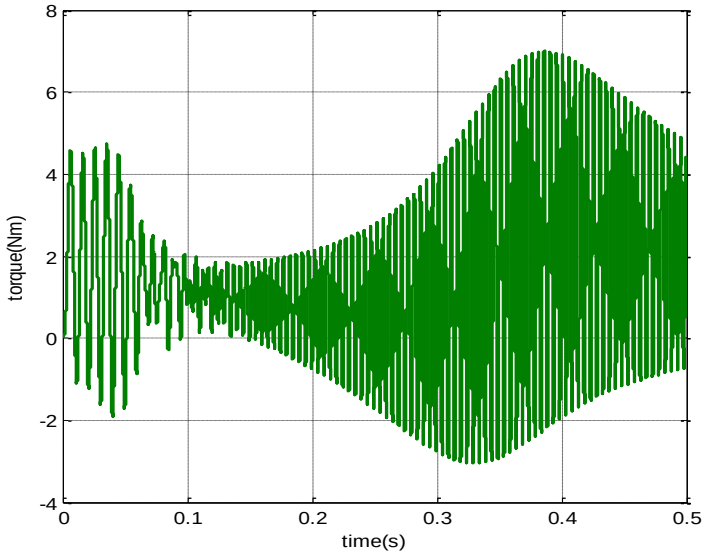


*Figure 5. 11:Torque pulastion for three phase induction motor*

## 5.5 The overall performance of the drive

The refrence speed of 1000 rpm is given intially the refrence speed is step raised to 1200 rpm,1400 rpm and 1500 rpm at t=1sec,2sec and 3sec,respectively.the actual speed very well follows the refrence as illustated in the following figures.

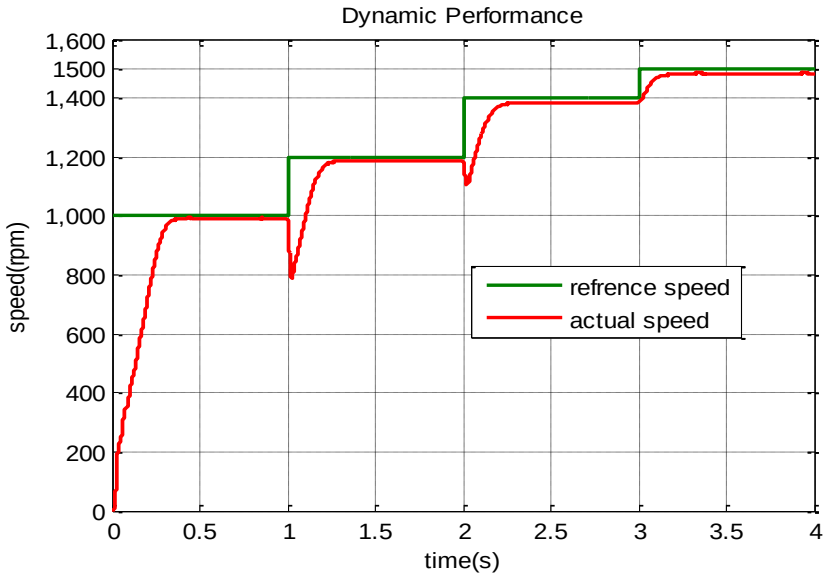


*Figure 5. 12: step Speed response for closed loop v/f control*

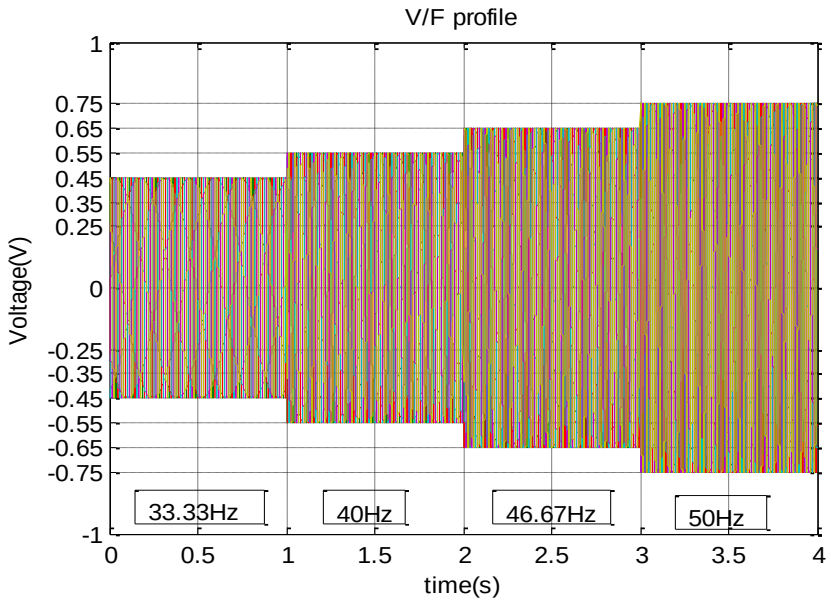


*Figure 5. 13: v/f response*

The simulation result is carried out to implement the open loop constant v/f control technique using the developed simulation model. The reference speed of 1500 rpm is given initially and then the load toque is applied after 1s duration. The actual speed very well follows the reference speed as illustrated below.

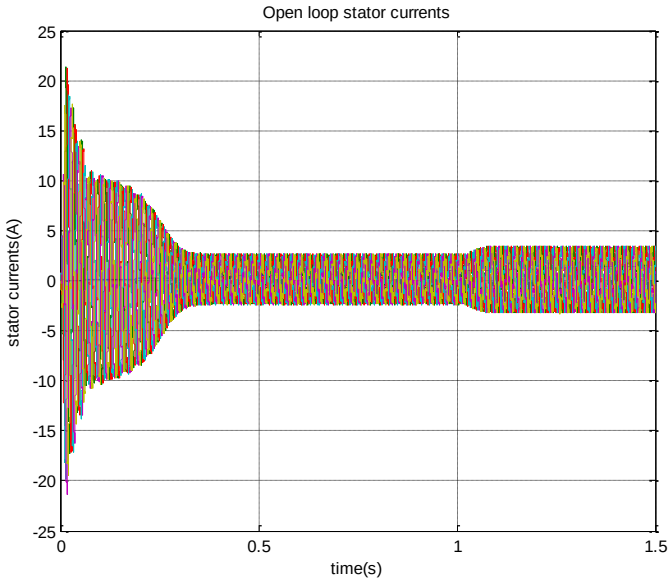


*Figure 5. 14:Open loop Stator Phase current*

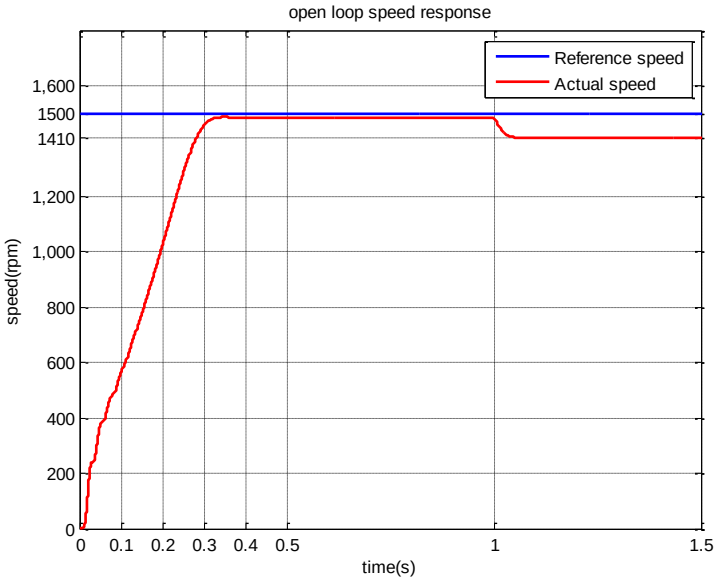


*Figure 5. 15:.Open loop speed response*

The simulation result is carried out to implement the closed loop constant v/f control technique using the developed simulation model. The machine is first started at no-load condition and the reference speed is given as 1500 rpm .once the machine attains the steady state speed, rated load of 8.33Nm is applied to the machine at t=1sec.

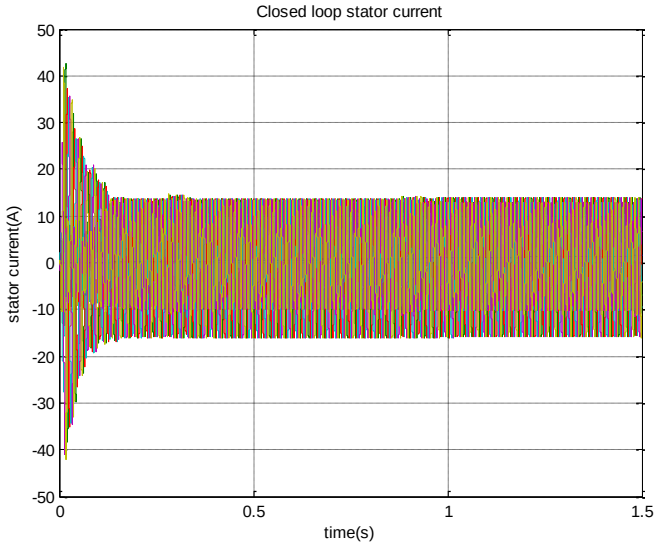


*Figure 5. 16:Closed loop Phase Stator current*

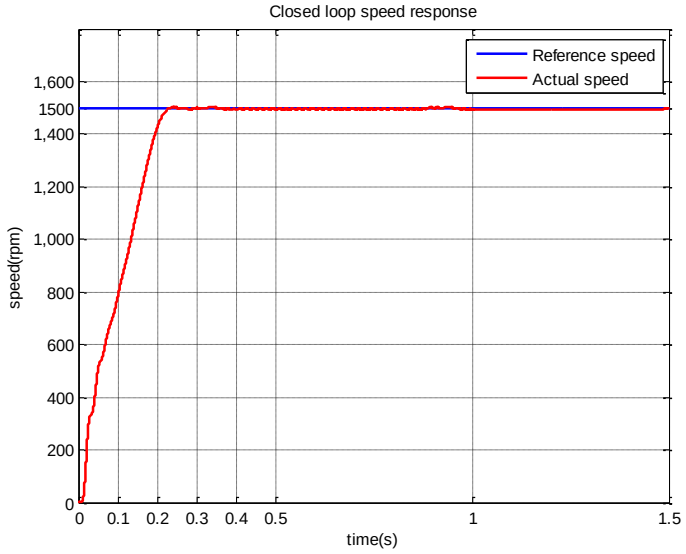


*Figure 5. 17:Closed loop speed response*

The steady state offset speed error is completely elimnated in the closed loop constant v/f control method.however a small overshoot in the speed response is observed ,this is due to the PIcontroller setting.the dip in speed due to loading is quickly recovered by the corrective PI controller.

Finally, some measures have been performed in closed-loop speed control with Volts/Hz control and slip regulation. Due to the slip regulation, the IM is able to rotate at the synchronous speed (1000 rpm at 33.33Hz,1200 rpm at 40 Hz,1400 rpm at 46.67 Hz and 1500 rpm at 50 Hz as P= 2) and, therefore, the torque-speed curves become vertical lines and constant at maximum torque for all speed variation as shown in Fig.5.23.

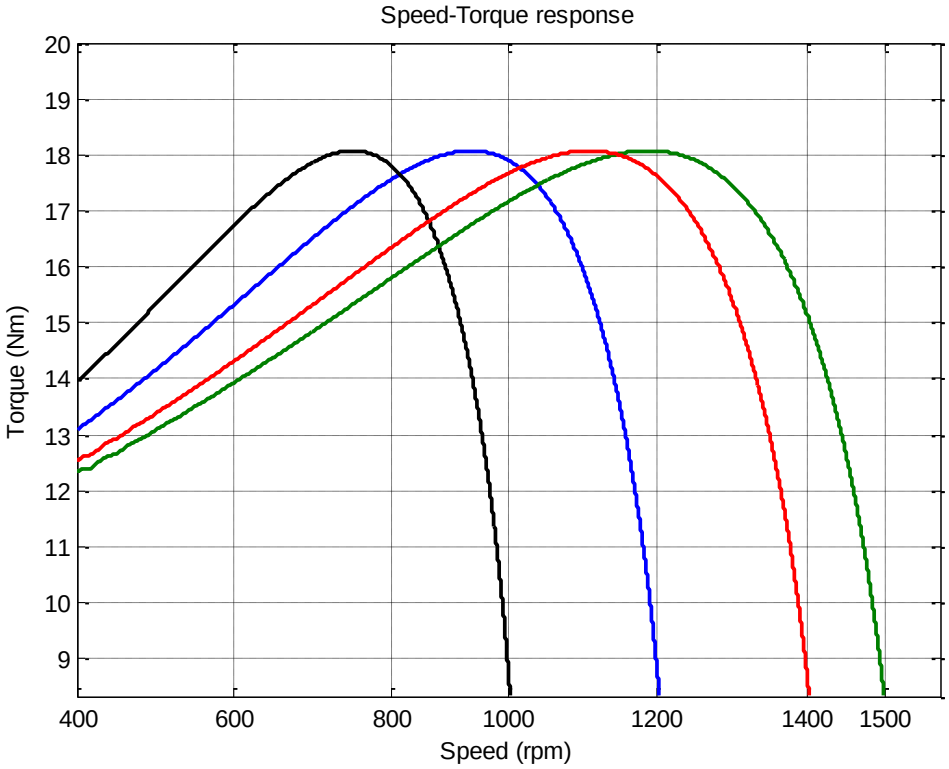


*Figure 5. 18: Speed Torque response in scalar control*

# CHAPTER SIX

## CONCLUSIONS, RECOMMENDATIONS AND FUTURE WORK

### 6.1 Conclusions

An Induction Motor was run with the help of a SVPWM Inverter without implementing any kind of speed control mechanisms and the various characteristic curves were obtained. It was observed that there were a lot of transient currents in the stator and rotor at the time of starting and they took some time to settle down to their steady-state values. The lower the stator resistance, the quicker the transients died down and hence, the stator resistance should be kept very low. In an uncontrolled Induction Motor, torque was observed to rise to a maximum value and then settle at the base value, while rotor speed was observed to rise to its rated value and remain constant there.

Closed-loop V/f Control used a PI Controller to process the error between the actual rotor speed and reference speed and used this to vary the supply frequency. The Voltage Source Inverter varied the magnitude of the Terminal Voltage accordingly so that the V/f ratio remained the same. It was observed that again the maximum torque remained constant across the speed range. Hence, the motor is fully utilized and successful speed control is achieved.

The first method of SVPWM technique uses vectors from large and middle sets. The simulation results show a considerable amount of low-order harmonic content (3rd) in the output phase voltages, which remains more or less constant (approximately 20%) throughout. The low-order harmonic content in the output phase voltages is due to the presence of zero-sequence components of large vectors. The second method uses only large set of space vectors and yields approximately 40% of the 3rdharmonic in output phase voltages, due to the presence of zero-sequence components of large vectors.

By comparing the work described in this thesis with the research objectives listed in section (1.3) it can be concluded that all the set goals have been achieved successfully.

### 6.2 Recommendation

In this thesis the scalar speed control of five phase induction motor is handled by assuming application areas where the dynamic performance of the machine is not coming into priority

However, there are different application areas where the dynamic performance of the drive system is so important and the instantaneous position of voltage, current and flux needed. This leads to the investigation of vector control instead of scalar control.

## 6.3 Future Work

This thesis explores the feasibility of v/f control of five-phase induction motor drive systems, fed from a five-phase SVPWM voltage source inverter. Since this drive structures are novel, it is believed that there is plenty of scope for further research. Some possible directions are the following:

- The multi-phase machines do not have perfect sinusoidal spatial distribution of windings, which leads to production of unwanted spatial air-gap harmonics. This aspect should be addressed in order to arrive at appropriate machine designs for five phase drive applications.
- An evaluation of the overall efficiency of the proposed drive systems for specific applications.
- Detailed study of the rating of the power switches for five-phase and VSIs aimed at supplying two series-connected machines.

# References

[1] Chen, S., Lipo, T. A., and Fitzgerald, D. (1996) Sources of induction motor gearing currents caused by PWM inverters.IEEE Trans. Ener. Conv., 11, 25–32.2. Klingshirn, E. A. (1983) High phase order induction motors (part I and II).IEEE Trans. Power App.Sys., PAS_102(1), 47–59.

[2] Pavithran, K. N., Parimelalagan, R., and Krishnamurthy, M. R. (1988) Studies on inverter-fed fivephase induction motor drive.IEEE Trans. On Power Elect., 3(2), 224–233.

[3] Zhang, X., Zhnag, C., Qiao, M., and Yu, F. (2008) Analysis and experiment of multi-phase induction motor drives for electrical propulsion.Proc. Int. Conf. Elect. Mach., ICEM, pp. 1251–1254.

[4] Xu, H., Toliyat, H. A., and Petersen, L. J. (2001) Rotor field oriented control of a five-phase induction motor with the combined fundamental and third harmonic injection.Proc. IEEE Applied Power Elec.Conf. APEC, Anaheim, CA, pp. 608–614.

[5] Iqbal, A. and Levi, E. (2005) Space vector modulation scheme for a five-phase voltage source inverter. Proc. Europ. Power Elect. Appl. Conf., EPE, Dresden, CD-ROM, paper 0006.

[6] Ojo,O.,Dong,G.,and Wu,Z.(2006) Pulsewidth modulation for five-phase converters based on device turn-on times.Proc. IEEE Ind. Appl. Soc. Ann. Mtg IAS, Tampa, FL, CD-ROM, paper IAS15, p. 7.

[7] Ryu, H. M., Kim, J. H., and Sul, S. K. (2005) Analysis of multi-phase space vector pulse width modulation based on multiple d-q space concept.IEEE Trans. Power Elect., 20(6), 1364–1371.

[8] de Silva, P. S. N., Fletcher, J. E., and Williams, B. W. (2004) Development of space vector modulation strategies for five-phase voltage source inverters. Proc. IEE Power Elect., Mach. Drives Conf.,PEMD, Edinburgh, pp. 650–655.

[9] Dujic, D., Jones, M., and Levi, E. (2009) Generalised space vector PWM for sinusoidal output voltage generation with multiphase voltage source inverters.Int. J. Ind. Elect. Drives, 1(1), 1–13.

[10] de Silva, P. S. N., Fletcher, J. E., and Williams, B. W. (2004) Development of space vector Modulation strategies for five-phase voltage source inverters.Proc. IEE Power Elect. Mach. Drives PEMD Conf.,Edinburgh, pp. 650–655.

[11] Iqbal, A. and Levi, E. (2006) Space vector PWM techniques for sinusoidal output voltage generation with a five-phase voltage source inverter.Elect. Power Comp. Syst.

[12] Duran, M. J., Toral, S., Barrero, F., and Levi, E. (2007) Real time implementation of multidimensional five-phase space vector pulse width modulation.Elect. Lett.43(17), 949–950.

[13] Ryu, H. M., Kim, J. H., and Sul, S. K. (2005) Analysis of multiphase space vector pulse-width modulation based on multiple d-q spaces concept.IEEE Trans. Power Elec., 20(6), 1364–1371.

[14] Zheng, L., Fletcher, J., Williams, B., and He, X. (2010) A novel direct torque control scheme for a sensorless five-phase induction motor drive. IEEE Trans. Ind. Elect. Issue 99 (on-line version available).

[15] Liliang, G. and Fletcher, J. E. (2010) A space vector switching strategy for a 3-level five-phaseinverter drives. IEEE Trans. Ind. Elect.(On-line version available).

[16] Singh, G. K. (2002) Multi-phase induction machine drive research: A survey.Elect. Power Syst. Res.,61, 139–147.

[17] Jones, M. and E. Levi, E. (2002) A literature survey of state-of-the-art in multiphase AC drives,Proc.37th Int. Univ. Power Eng. Conf. UPEC, Stafford, UK, pp. 505–510.

[18] Levi, E., Bojoi, R., Profumo, F., Toliyat, H. A., and Williamson, S. (2007) Multi-phase induction motor drives: A technology status review.IET Elect. Power Appl., 1(4), 489–516.

[19] Levi, E. (2008) Guest editorial.IEEE Trans. Ind. Elect., 55(5), 1891–1892.

[20] Levi, E. (2008) Multi-phase machines for variable speed applications.IEEE Trans. Ind. Elect.,55(5),1893–1909.

[21] Toliyat,H.A.,Rahimian,M.M.,and Lipo,T.A.(1991) dq modeling of five-phase synchronous reluctance machines including third harmonic air-gap mmf.Proc. IEEE Ind. Appl. Soc. Ann. Mtg, pp. 231–237.

[22] Jones, M., Levi, E. and Iqbal, A., (2005), Vector control of a five-phase series-connected two motor drive using synchronous current controllers, Electric Power Components and Systems, vol. 33, no. 4, pp. 411-430.

# APPENDIX

## Appendix A: Five phase induction motor model

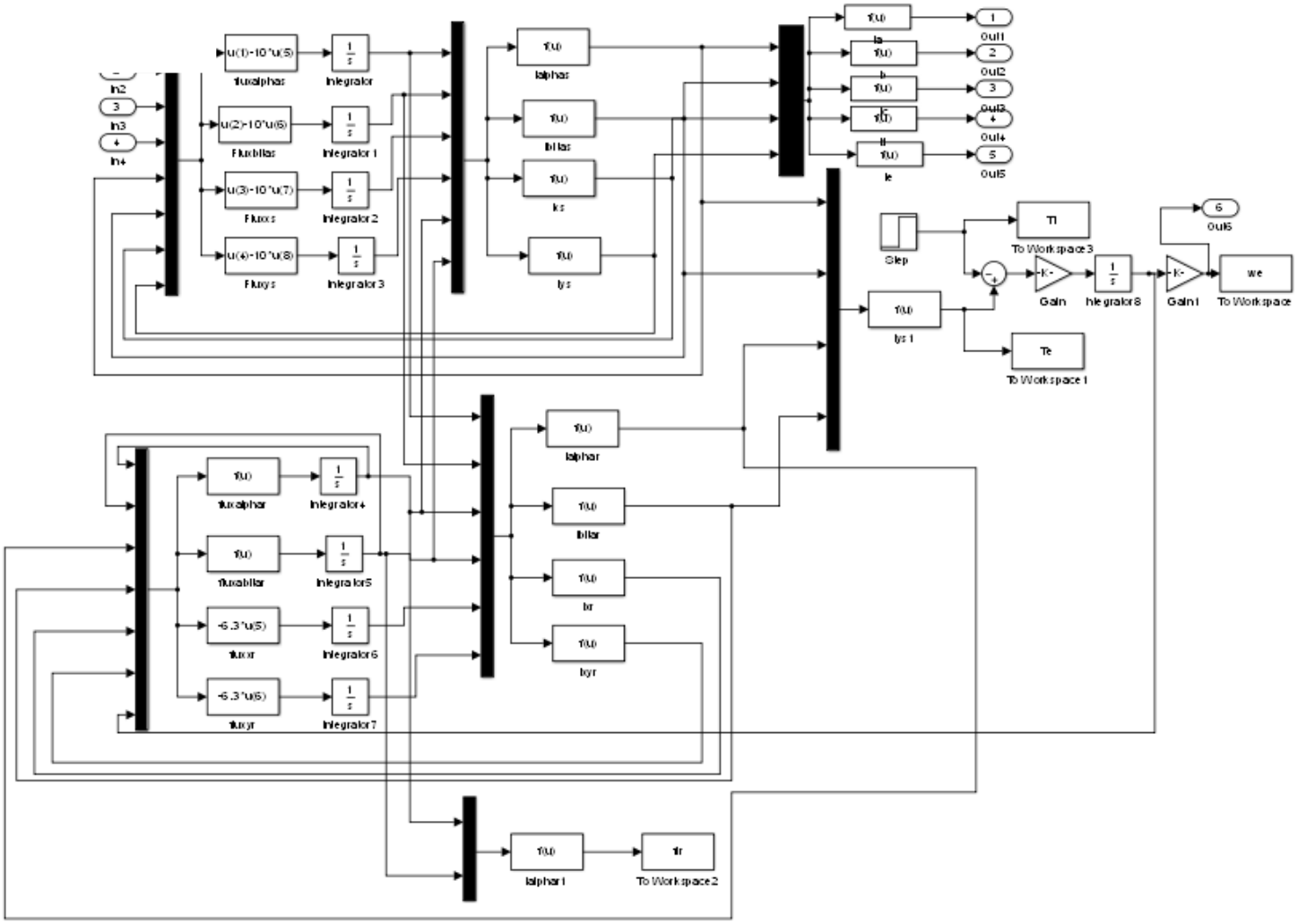


*Figure A. 1: five phase induction motor model*

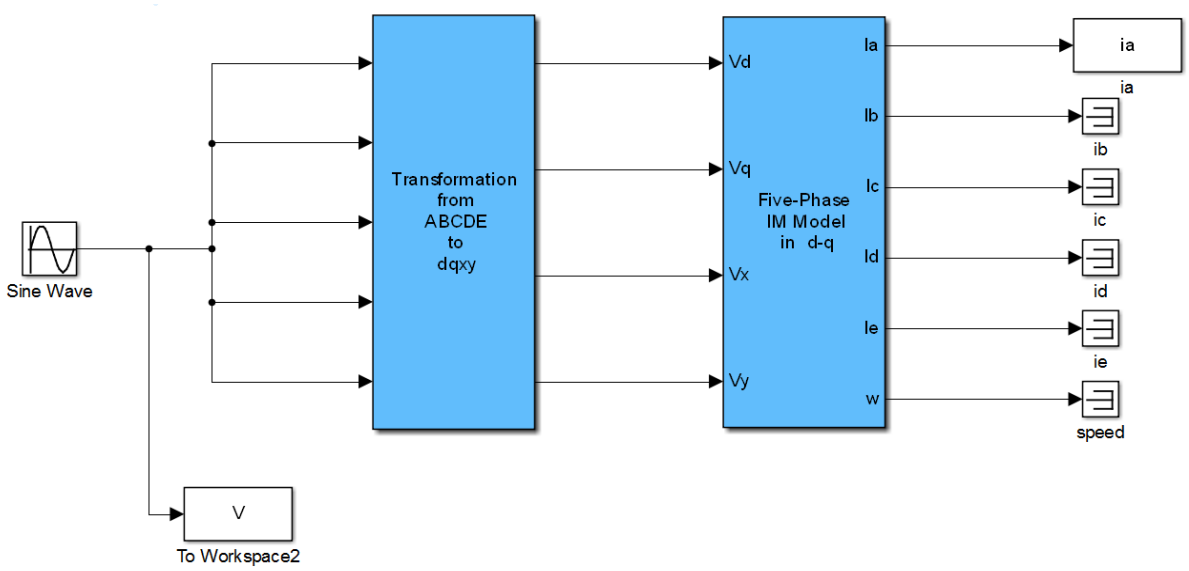


*Figure A. 2: complete transformation of d-q model*

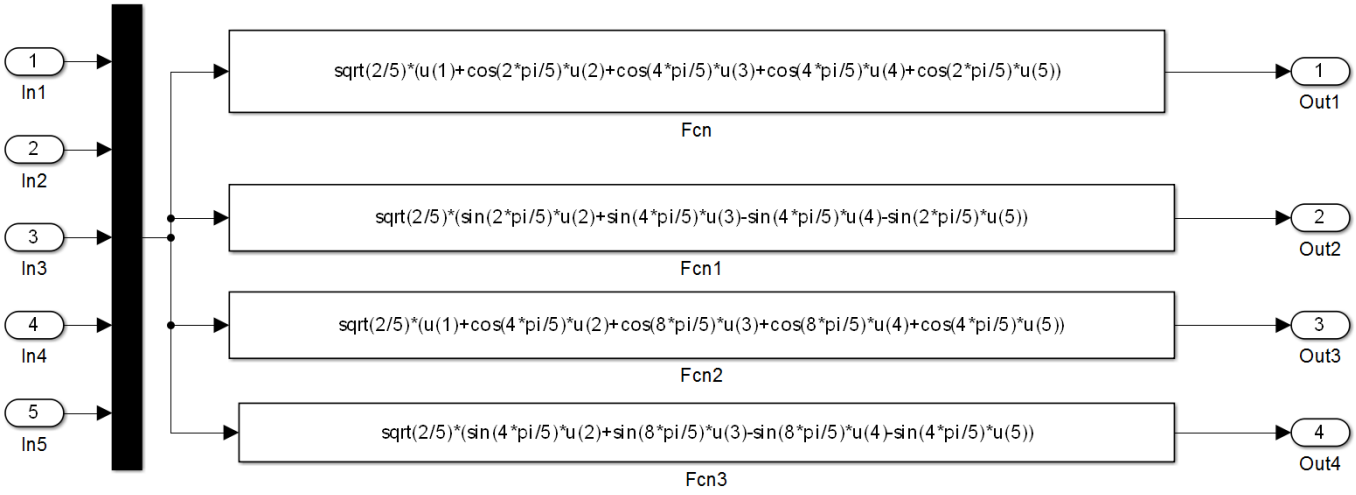


*Figure A. 3: transformation of d-q model*

# Appendix B: v/f block

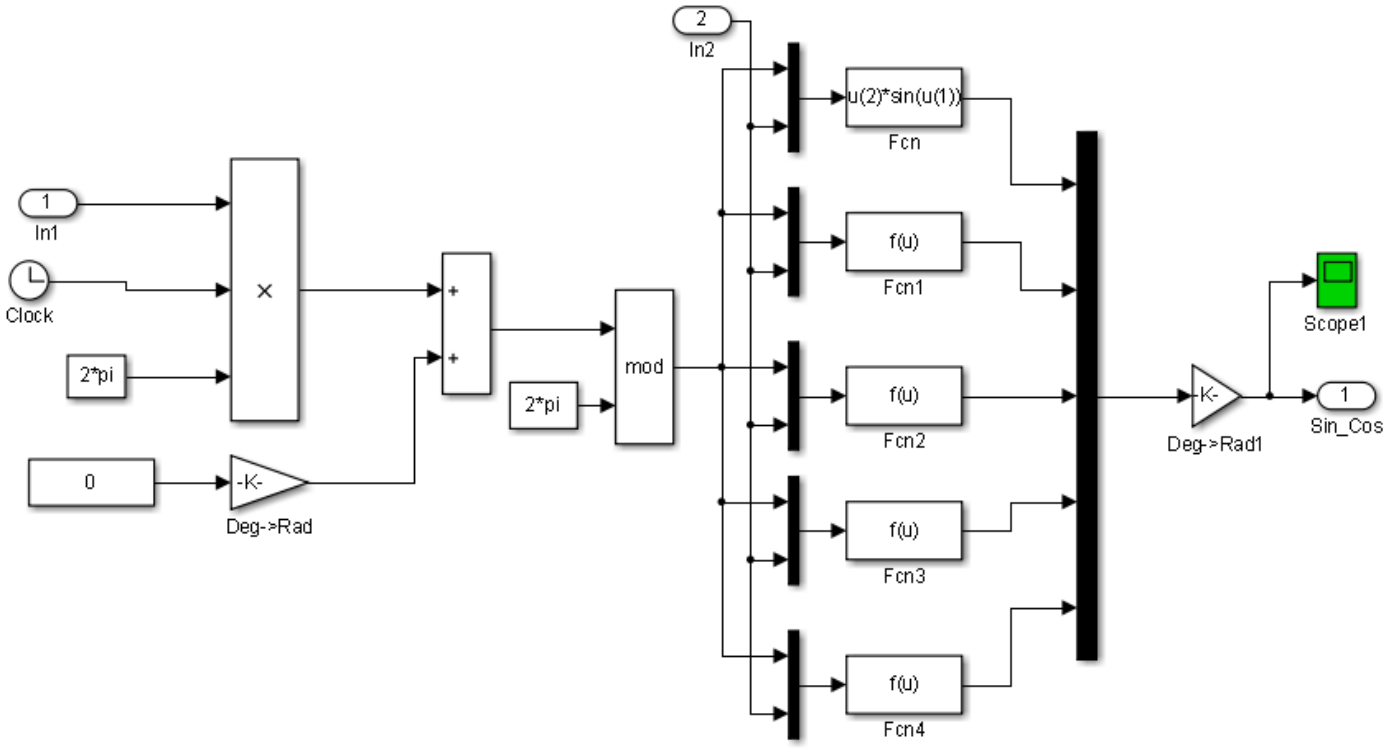


*Figure B. 1: Variable voltage variable frequency block*

## Appendix C: Closed loop v/f speed Control scheme

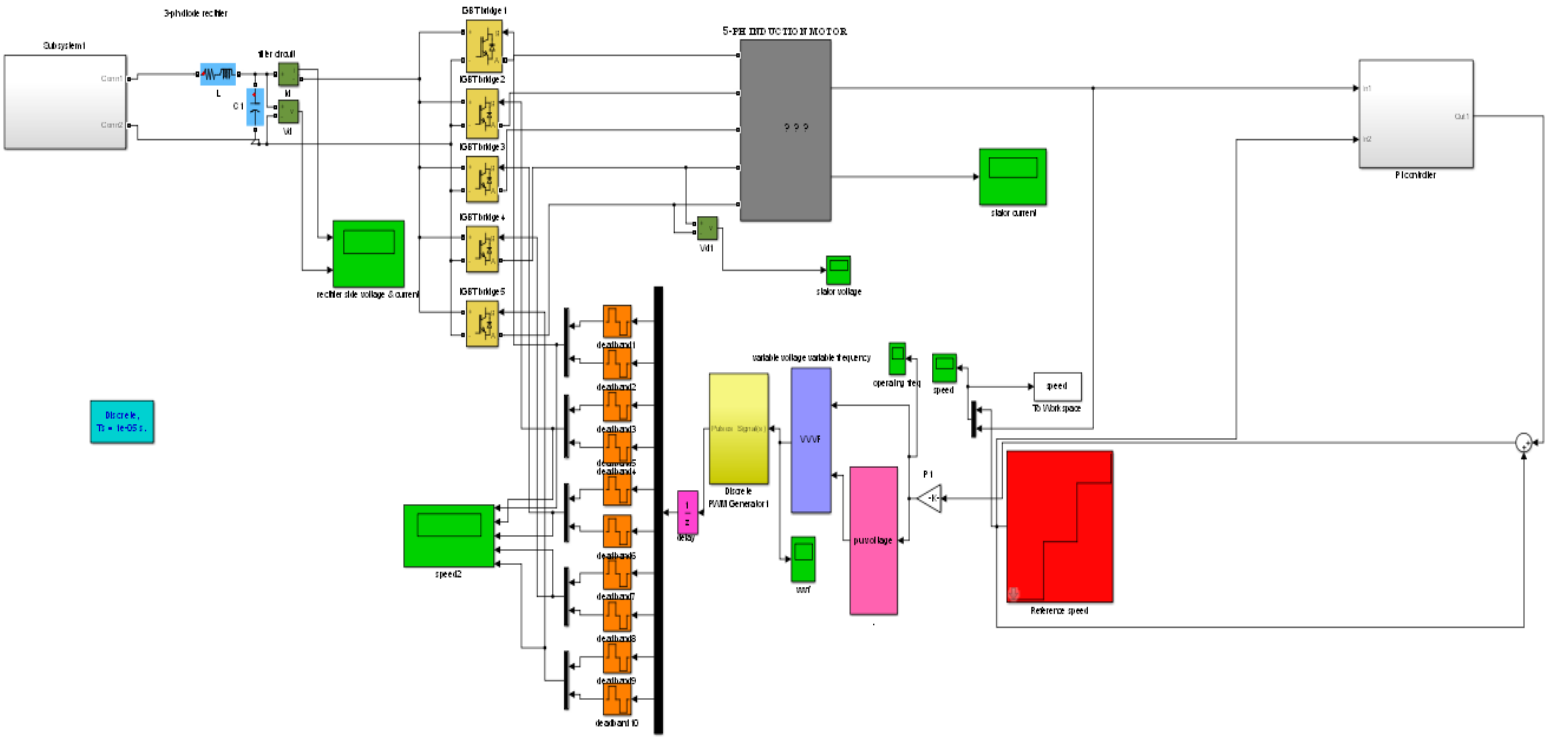


*Figure C. 1: V/F Drive system*

# Appendix D: SVPWM implementation

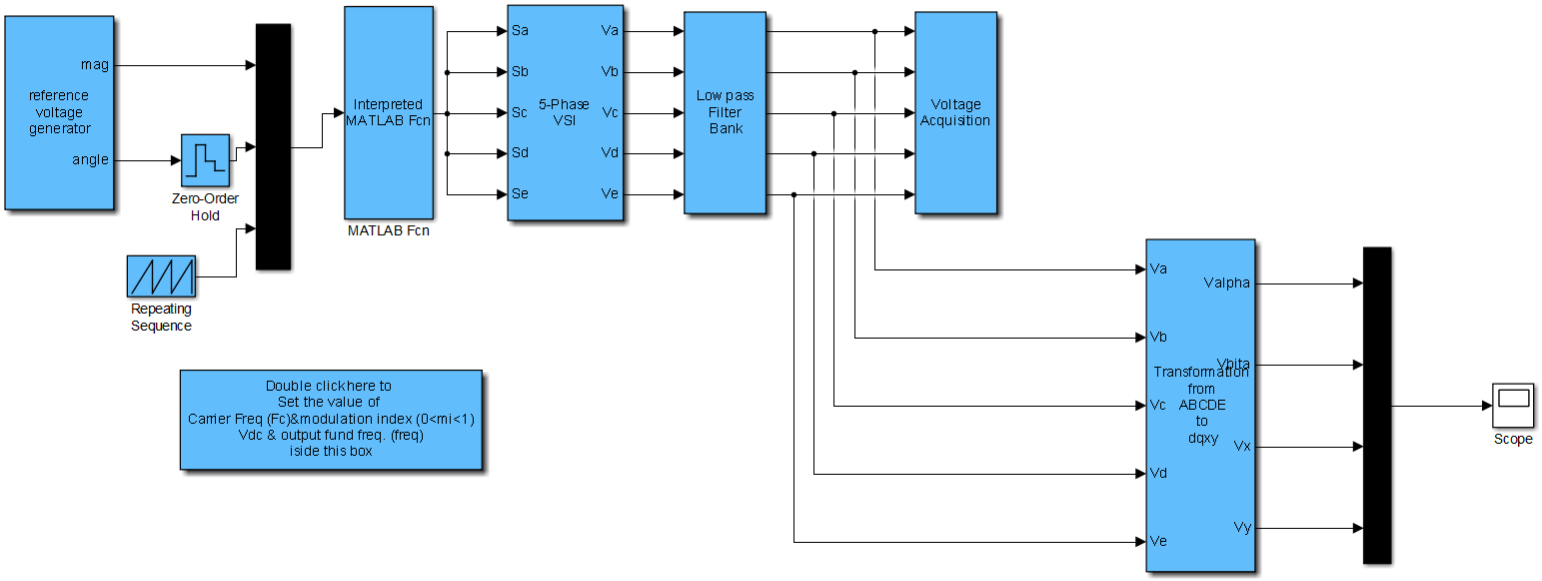


*Figure D. 1: SVPWM*

## Appendix E: SVPWM code for four vector application

```
function [sf]=svpwm(u)

    ts=0.0002;  vdc=200; k=1.618;

    x=u(2);

    m=5*u(1)*ts/(2*vdc*sin(pi/5)*(1+k^2));

    y=u(3);


    % sector I
    if (x>=0) && (x<pi/5)

        ta1=m*k*sin(pi/5-x);
        ta2=m*sin(pi/5-x);
        tb1=m*k*sin(x);
        tb2=m*sin(x);
        t0=ts-ta1-ta2-tb1-tb2;

        t1=[t0/4 ta2/2 tb1/2 ta1/2 tb2/2 t0/2 tb2/2 ta1/2 tb1/2 ta2/2 t0/4];

        t1=cumsum(t1);

        v1=[0  1  1  1  1 1  1  1  1  1 0];
        v2=[0 0  1  1  1 1  1  1  1 0 0];
        v3=[0 0 0 0  1 1  1 0 0 0 0];
        v4=[0 0 0 0 0 1 0 0 0 0 0];
        v5=[0 0 0  1  1 1  1  1 0 0 0];


        for j=1:11
            if(y<t1(j))
                break
            end
        end

        sa=v1(j);
        sb=v2(j);
        sc=v3(j);
        sd=v4(j);
        se=v5(j);

    end

    % sector II
    if (x>=pi/5) && (x<2*pi/5)
```

```
        adv= x-pi/5;

        ta1=m*k*sin(pi/5-adv);
        ta2=m*sin(pi/5-adv);
        tb1=m*k*sin(adv);
        tb2=m*sin(adv);
        t0=ts-ta1-ta2-tb1-tb2;

        t1=[t0/4 tb2/2 ta1/2 tb1/2 ta2/2 t0/2 ta2/2 tb1/2 ta1/2 tb2/2 t0/4];
        t1=cumsum(t1);

        v1=[0 0  1  1  1 1  1  1  1 0 0];
        v2=[0  1  1  1  1 1  1  1  1  1 0];
        v3=[0 0 0  1  1 1  1  1 0 0 0];
        v4=[0 0 0 0 0 1 0 0 0 0 0];
        v5=[0 0 0 0  1 1  1 0 0 0 0];

    for j=1:11
        if(y<t1(j))
            break
        end
    end

        sa=v1(j);
        sb=v2(j);
        sc=v3(j);
        sd=v4(j);
        se=v5(j);
    end

    %sector III

    if (x>=2*pi/5) && (x<3*pi/5)

        adv=x-2*pi/5;

        ta1=m*k*sin(pi/5-adv);
        ta2=m*sin(pi/5-adv);
        tb1=m*k*sin(adv);
        tb2=m*sin(adv);
        t0=ts-ta1-ta2-tb1-tb2;

        t1=[t0/4 ta2/2 tb1/2 ta1/2 tb2/2 t0/2 tb2/2 ta1/2 tb1/2 ta2/2 t0/4];

        t1=cumsum(t1);

        v1=[0 0 0  1  1  1  1  1 0 0 0];
        v2=[0  1  1  1  1  1  1  1  1  1 0];
        v3=[0 0  1  1  1  1  1  1  1 0 0];
        v4=[0 0 0 0  1  1  1 0 0 0 0];
        v5=[0 0 0 0 0  1 0 0 0 0 0];

    for j=1:11
        if(y<t1(j))
```

```
            break
        end
    end

        sa=v1(j);
        sb=v2(j);
        sc=v3(j);
        sd=v4(j);
        se=v5(j);
end

    %sector IV

    if (x>=3*pi/5) && (x<4*pi/5)

                adv = x-3*pi/5;

        ta1=m*k*sin(pi/5-adv);
        ta2=m*sin(pi/5-adv);
        tb1=m*k*sin(adv);
        tb2=m*sin(adv);
        t0=ts-ta1-ta2-tb1-tb2;


        t1=[t0/4 tb2/2 ta1/2 tb1/2 ta2/2 t0/2 ta2/2 tb1/2 ta1/2 tb2/2 t0/4];
        t1=cumsum(t1);

        v1=[0 0 0 0  1 1  1 0 0 0 0];
        v2=[0 0  1  1  1 1  1  1  1 0 0];
        v3=[0  1  1  1  1 1  1  1  1  1 0];
        v4=[0 0 0  1  1 1  1  1 0 0 0];
        v5=[0 0 0 0 0 1 0 0 0 0 0];

    for j=1:11
        if(y<t1(j))
            break
        end
    end

        sa=v1(j);
        sb=v2(j);
        sc=v3(j);
        sd=v4(j);
        se=v5(j);

end

    % sector V

    if (x>=4*pi/5) && (x<=pi)

        adv = x-4*pi/5;

        ta1=m*k*sin(pi/5-adv);
```

```
        ta2=m*sin(pi/5-adv);
        tb1=m*k*sin(adv);
        tb2=m*sin(adv);
        t0=ts-ta1-ta2-tb1-tb2;

        t1=[t0/4 ta2/2 tb1/2 ta1/2 tb2/2 t0/2 tb2/2 ta1/2 tb1/2 ta2/2 t0/4];

        t1=cumsum(t1);

        v1=[0 0 0 0 0 1 0 0 0 0 0];
        v2=[0 0 0  1  1 1  1  1 0 0 0];
        v3=[0  1  1  1  1 1  1  1  1  1 0];
        v4=[0 0  1  1  1 1  1  1  1 0 0];
        v5=[0 0 0 0  1 1  1 0 0 0 0];

    for j=1:11
        if(y<t1(j))
            break
        end
    end

    sa=v1(j);
    sb=v2(j);
    sc=v3(j);
    sd=v4(j);
    se=v5(j);

end

    %Sector VI

    if (x>=-pi) && (x<-4*pi/5)

        adv = x+pi;

        ta1=m*k*sin(pi/5-adv);
        ta2=m*sin(pi/5-adv);
        tb1=m*k*sin(adv);
        tb2=m*sin(adv);
        t0=ts-ta1-ta2-tb1-tb2;


        t1=[t0/4 tb2/2 ta1/2 tb1/2 ta2/2 t0/2 ta2/2 tb1/2 ta1/2 tb2/2 t0/4];
        t1=cumsum(t1);

        v1=[0 0 0 0 0 1 0 0 0 0 0];
        v2=[0 0 0 0  1 1  1 0 0 0 0];
        v3=[0 0  1  1  1 1  1  1  1 0 0];
        v4=[0  1  1  1  1 1  1  1  1  1 0];
        v5=[0 0 0  1  1 1  1  1 0 0 0];

    for j=1:11
        if(y<t1(j))
            break
```

```
        end
    end
    sa=v1(j);
    sb=v2(j);
    sc=v3(j);
    sd=v4(j);
    se=v5(j);

end
    % sector VII

    if (x>=-4*pi/5) && (x<-3*pi/5)

        adv = x+4*pi/5;

        ta1=m*k*sin(pi/5-adv);
        ta2=m*sin(pi/5-adv);
        tb1=m*k*sin(adv);
        tb2=m*sin(adv);
        t0=ts-ta1-ta2-tb1-tb2;

        t1=[t0/4 ta2/2 tb1/2 ta1/2 tb2/2 t0/2 tb2/2 ta1/2 tb1/2 ta2/2 t0/4];

        t1=cumsum(t1);

        v1=[0 0 0 0  1 1  1 0 0 0 0];
        v2=[0 0 0 0 0 1 0 0 0 0 0];
        v3=[0 0 0  1  1 1  1  1 0 0 0];
        v4=[0  1  1  1  1 1  1  1  1  1 0];
        v5=[0 0  1  1  1 1  1  1  1 0 0];

    for j=1:11
        if(y<t1(j))
            break
        end
    end
    sa=v1(j);
    sb=v2(j);
    sc=v3(j);
    sd=v4(j);
    se=v5(j);

end

    %sector VIII

    if (x>=-3*pi/5) && (x<-2*pi/5)

        adv = x+3*pi/5;

        ta1=m*k*sin(pi/5-adv);
        ta2=m*sin(pi/5-adv);
        tb1=m*k*sin(adv);
        tb2=m*sin(adv);
```

```
        t0=ts-ta1-ta2-tb1-tb2;


        t1=[t0/4 tb2/2 ta1/2 tb1/2 ta2/2 t0/2 ta2/2 tb1/2 ta1/2 tb2/2 t0/4];
        t1=cumsum(t1);

        v1=[0 0 0  1  1 1  1  1 0 0 0];
        v2=[0 0 0 0 0 1 0 0 0 0 0];
        v3=[0 0 0 0  1 1  1 0 0 0 0];
        v4=[0 0  1  1  1 1  1  1  1 0 0];
        v5=[0  1  1  1  1 1  1  1  1  1 0];

    for j=1:11
        if(y<t1(j))
            break
        end
    end
    sa=v1(j);
    sb=v2(j);
    sc=v3(j);
    sd=v4(j);
    se=v5(j);

end

    % sector IX

    if (x>=-2*pi/5) && (x<-pi/5)

        adv = x+2*pi/5;

        ta1=m*k*sin(pi/5-adv);
        ta2=m*sin(pi/5-adv);
        tb1=m*k*sin(adv);
        tb2=m*sin(adv);
        t0=ts-ta1-ta2-tb1-tb2;

        t1=[t0/4 ta2/2 tb1/2 ta1/2 tb2/2 t0/2 tb2/2 ta1/2 tb1/2 ta2/2 t0/4];

        t1=cumsum(t1);

        v1=[0 0  1  1  1 1  1  1  1 0 0];
        v2=[0 0 0 0  1 1  1 0 0 0 0];
        v3=[0 0 0 0 0 1 0 0 0 0 0];
        v4=[0 0 0  1  1 1  1  1 0 0 0];
        v5=[0  1  1  1  1 1  1  1  1  1 0];

    for j=1:11
        if(y<t1(j))
            break
        end
    end
    sa=v1(j);
    sb=v2(j);
```

```
    sc=v3(j);
    sd=v4(j);
    se=v5(j);

end

    % sector X

    if (x>=-pi/5) && (x<0)

        adv = x+pi/5;

        ta1=m*k*sin(pi/5-adv);
        ta2=m*sin(pi/5-adv);
        tb1=m*k*sin(adv);
        tb2=m*sin(adv);
        t0=ts-ta1-ta2-tb1-tb2;


        t1=[t0/4 tb2/2 ta1/2 tb1/2 ta2/2 t0/2 ta2/2 tb1/2 ta1/2 tb2/2 t0/4];
        t1=cumsum(t1);

        v1=[0  1  1  1  1 1  1  1  1  1 0];
        v2=[0 0 0  1  1 1  1  1 0 0 0];
        v3=[0 0 0 0 0 1 0 0 0 0 0];
        v4=[0 0 0 0  1 1  1 0 0 0 0];
        v5=[0 0  1  1  1 1  1  1  1 0 0];

    for j=1:11
        if(y<t1(j))
            break
        end
    end
    sa=v1(j);
    sb=v2(j);
    sc=v3(j);
    sd=v4(j);
    se=v5(j);

end


   sf=[sa,sb, sc, sd, se];
```

**Appendix F: SVPWM code for two vector application**

```
function [sf]=sp5onlyl(u)
ts=0.0002;  vdc=1;
    %peak_phase_max = ((2/5)*vdc*2*cos(pi/5)*cos(pi/10));

    x=u(2);


    y=u(3);

    VL=0.8*cos(pi/5)*vdc;
    mag=(u(1)/(VL*sin(pi/5)))*ts;
    %1.618123 = 1/(2*sin(pi/10));



    % sector I
    if (x>=0) && (x<pi/5)

        ta = mag * sin(pi/5-x);
        tb = mag * sin(x);
        t0 =(ts-ta-tb);

        t1=[t0/4 tb/2 ta/2 t0/2 ta/2 tb/2 t0/4];

        t1=cumsum(t1);

        v1=[0  1  1 1  1  1 0];
        v2=[0  1  1 1  1  1 0];
        v3=[0 0 0 1 0 0 0];
        v4=[0 0 0 1 0 0 0];
        v5=[0 0  1 1  1 0 0];


        for j=1:7
            if(y<t1(j))
                break
            end
        end

        sa=v1(j);
        sb=v2(j);
        sc=v3(j);
        sd=v4(j);
        se=v5(j);

    end

    % sector II
    if (x>=pi/5) && (x<2*pi/5)

        adv= x-pi/5;
```

```
    ta = mag * sin(pi/5-adv);
    tb = mag * sin(adv);
    t0 =(ts-ta-tb);

    t1=[t0/4 ta/2 tb/2 t0/2 tb/2 ta/2 t0/4];
    t1=cumsum(t1);

    v1=[0  1  1 1  1  1 0];
    v2=[0  1  1 1  1  1 0];
    v3=[0 0  1 1  1 0 0];
    v4=[0 0 0 1 0 0 0];
    v5=[0 0 0 1 0 0 0];

for j=1:7
    if(y<t1(j))
        break
    end
end

    sa=v1(j);
    sb=v2(j);
    sc=v3(j);
    sd=v4(j);
    se=v5(j);
end

%sector III

if (x>=2*pi/5) && (x<3*pi/5)

    adv=x-2*pi/5;

    ta = mag * sin(pi/5-adv);
    tb = mag * sin(adv);
    t0 =(ts-ta-tb);

    t1=[t0/4 tb/2 ta/2 t0/2 ta/2 tb/2 t0/4];

    t1=cumsum(t1);

    v1=[0 0  1 1  1 0 0];
    v2=[0  1  1 1  1  1 0];
    v3=[0  1  1 1  1  1 0];
    v4=[0 0 0 1 0 0 0];
    v5=[0 0 0 1 0 0 0];

for j=1:7
    if(y<t1(j))
        break
    end
end

    sa=v1(j);
```

```
        sb=v2(j);
        sc=v3(j);
        sd=v4(j);
        se=v5(j);
end

    %sector IV

    if (x>=3*pi/5) && (x<4*pi/5)

                adv = x-3*pi/5;

        ta= mag * sin(pi/5 - adv);
        tb = mag * sin(adv);
        t0 =(ts-ta-tb);

        t1=[t0/4 ta/2 tb/2 t0/2 tb/2 ta/2 t0/4];
        t1=cumsum(t1);

        v1=[0 0 0 1 0 0 0];
        v2=[0  1  1 1  1  1 0];
        v3=[0  1  1 1  1  1 0];
        v4=[0 0  1 1  1 0 0];
        v5=[0 0 0 1 0 0 0];

    for j=1:7
        if(y<t1(j))
            break
        end
    end

        sa=v1(j);
        sb=v2(j);
        sc=v3(j);
        sd=v4(j);
        se=v5(j);

end

    % sector V

    if (x>=4*pi/5) && (x<=pi)

        adv = x-4*pi/5;

        ta = mag * sin(pi/5-adv);
        tb = mag * sin(adv);
        t0 =(ts-ta-tb);

        t1=[t0/4 tb/2 ta/2 t0/2 ta/2 tb/2 t0/4];

        t1=cumsum(t1);

        v1=[0 0 0 1 0 0 0];
```

```
        v2=[0 0  1 1  1 0 0];
        v3=[0  1  1 1  1  1 0];
        v4=[0  1  1 1  1  1 0];
        v5=[0 0 0 1 0 0 0];

    for j=1:7
        if(y<t1(j))
            break
        end
    end

    sa=v1(j);
    sb=v2(j);
    sc=v3(j);
    sd=v4(j);
    se=v5(j);

end

    %Sector VI

    if (x>=-pi) && (x<-4*pi/5)

        adv = x+pi;

        ta = mag * sin(pi/5-adv);
        tb = mag * sin(adv);
        t0 =(ts-ta-tb);

        t1=[t0/4 ta/2 tb/2 t0/2 tb/2 ta/2 t0/4];
        t1=cumsum(t1);

        v1=[0 0 0 1 0 0 0];
        v2=[0 0 0 1 0 0 0];
        v3=[0  1  1 1  1  1 0];
        v4=[0  1  1 1  1  1 0];
        v5=[0 0  1 1  1 0 0];
    for j=1:7
        if(y<t1(j))
            break
        end
    end
    sa=v1(j);
    sb=v2(j);
    sc=v3(j);
    sd=v4(j);
    se=v5(j);

end
    % sector VII

    if (x>=-4*pi/5) && (x<-3*pi/5)

        adv = x+4*pi/5;
```

```
        ta = mag * sin(pi/5-adv);
        tb = mag * sin(adv);
        t0 =(ts-ta-tb);

        t1=[t0/4 tb/2 ta/2 t0/2 ta/2 tb/2 t0/4];

        t1=cumsum(t1);

        v1=[0 0 0 1 0 0 0];
        v2=[0 0 0 1 0 0 0];
        v3=[0 0  1 1  1 0 0];
        v4=[0  1  1 1  1  1 0];
        v5=[0  1  1 1  1  1 0];

    for j=1:7
        if(y<t1(j))
            break
        end
    end
    sa=v1(j);
    sb=v2(j);
    sc=v3(j);
    sd=v4(j);
    se=v5(j);

end

    %sector VIII

    if (x>=-3*pi/5) && (x<-2*pi/5)

        adv = x+3*pi/5;

        ta = mag * sin(pi/5-adv);
        tb = mag * sin(adv);
        t0 =(ts-ta-tb);

        t1=[t0/4 ta/2 tb/2 t0/2 tb/2 ta/2 t0/4];
        t1=cumsum(t1);

        v1=[0 0  1 1  1 0 0];
        v2=[0 0 0 1 0 0 0];
        v3=[0 0 0 1 0 0 0];
        v4=[0  1  1 1  1  1 0];
        v5=[0  1  1 1  1  1 0];

    for j=1:7
        if(y<t1(j))
            break
        end
    end
    sa=v1(j);
    sb=v2(j);
```

```
    sc=v3(j);
    sd=v4(j);
    se=v5(j);

end

    % sector IX

    if (x>=-2*pi/5) && (x<-pi/5)

        adv = x+2*pi/5;

        ta = mag * sin(pi/5-adv);
        tb = mag * sin(adv);
        t0 =(ts-ta-tb);

        t1=[t0/4 tb/2 ta/2 t0/2 ta/2 tb/2 t0/4];

        t1=cumsum(t1);

        v1=[0  1  1 1  1  1 0];
        v2=[0 0 0 1 0 0 0];
        v3=[0 0 0 1 0 0 0];
        v4=[0 0  1 1  1 0 0];
        v5=[0  1  1 1  1  1 0];

    for j=1:7
        if(y<t1(j))
            break
        end
    end
    sa=v1(j);
    sb=v2(j);
    sc=v3(j);
    sd=v4(j);
    se=v5(j);

end

    % sector X

    if (x>=-pi/5) && (x<0)

        adv = x+pi/5;

        ta = mag * sin(pi/5-adv);
        tb = mag * sin(adv);
        t0 =(ts-ta-tb);

        t1=[t0/4 ta/2 tb/2 t0/2 tb/2 ta/2 t0/4];
        t1=cumsum(t1);

        v1=[0  1  1 1  1  1 0];
        v2=[0 0  1 1  1 0 0];
```

```
        v3=[0 0 0 1 0 0 0];
        v4=[0 0 0 1 0 0 0];
        v5=[0  1  1 1  1  1 0];

    for j=1:7
        if(y<t1(j))
            break
        end
    end
    sa=v1(j);
    sb=v2(j);
    sc=v3(j);
    sd=v4(j);
    se=v5(j);

end


   sf=[sa, sb, sc, sd, se];
```

# Declaration

I, the undersigned, declare that this thesis work is my original work, has not been presented for a degree in this or any other universities, and all sources of materials used for the thesis work have been fully acknowledged.

Mesfin Tilahune Tessema _____
Name Signature

Place: Addis Ababa Institute of Technology, AAiT
Addis Ababa University, AAU
Addis Ababa,
Ethiopia.

Submitted in: March, 2015.

This thesis has been submitted for examination with my approval as a university advisor.

Dr. Mengesha Mamo _____
Name Signature